SEPIOLITE EMBEDDED NANOCOMPOSITE CARTRIDGES FOR HEAVY METAL REMOVAL FROM WATER

SULARDAN AĞIR METAL ARITIMI İÇİN SEPİYOLİT İÇERİKLİ NANOKOMPOZİT KARTUŞLAR

ÇAĞTAY ÇİÇEK

Assoc. Prof. AYŞE MÜGE ANDAÇ ÖZDİL
Supervisor

Submitted to
Graduate School of Science and Engineering of Hacettepe University
as a Partial Fulfillment to the Requirements
for the Award of the Degree of Master of Science in Environmental Engineering

2020

YAYINLAMA VE FİKRİ MÜLKİYET HAKLARI BEYANI

Enstitü tarafından onaylanan lisansüstü tezimin tamamını veya herhangi bir kısmını, basılı (kağıt) ve elektronik formatta arşivleme ve aşağıda verilen koşullarla kullanıma açma iznini Hacettepe Üniversitesi'ne verdiğimi bildiririm. Bu izinle Üniversiteye verilen kullanım hakları dışındaki tüm fikri mülkiyet haklarım bende kalacak, tezimin tamamının ya da bir bölümünün gelecekteki çalışmalarda (makale, kitap, lisans ve patent vb.) kullanım hakları bana ait olacaktır.

Tezin kendi orijinal çalışmam olduğunu, başkalarının haklarını ihlal etmediğimi ve tezimin tek yetkili sahibi olduğumu beyan ve taahhüt ederim. Tezimde yer alan telif hakkı bulunan ve sahiplerinden yazılı izin alınarak kullanması zorunlu metinlerin yazılı izin alarak kullandığımı ve istenildiğinde suretlerini üniversiteye teslim etmeyi taahhüt ederim.

Yükseköğretim Kurulu tarafından yayınlanan "Lisansüstü Tezlerin Elektronik Ortamda Toplanması, Düzenlenmesi ve Erişime Açılmasına İlişkin Yönerge" kapsamında tezim aşağıda belirtilen koşullar haricince YÖK Ulusal Tez Merkezi / H.Ü. Kütüphaneleri Açık Erişim Sistemi'nde erişime açılır.

□ Enstitü yönetim kurulu kararı ile tezimin erişime açılması mezuniyet tarihimden itibaren 2 yıl ertelenmiştir.

□ Enstitü yönetim kurulu gerekçeli kararı ile tezimin erişime açılması mezuniyet tarihimden itibaren ....ay ertelenmiştir.

□ Tezim ile ilgili gizlilik kararı verilmiştir.

19/06/2020

Çağtay ÇİÇEK

ETHICS

In this thesis study, prepared in accordance with the spelling rules of Institute of Graduate School of Science and Engineering of Hacettepe University,

I declare that,

- all the information and documents have been obtained in the base of the academic rules,
- all audio-visual and written information and results have been presented according to the rules of scientific ethics,
- in case of using other works, related studies have been cited in accordance with the scientific standards,
- all cited studies have been fully referenced,
- I did not do any distortion in the data set,
- and any part of this thesis has not been presented as another thesis study at this or any other university.

19/06/2020

Çağtay ÇİÇEK

ABSTRACT

SEPIOLITE EMBEDDED NANOCOMPOSITE CARTRIDGES FOR HEAVY METAL REMOVAL FROM WATER

Çağtay ÇİÇEK

Master of Science, Department of Environmental Engineering
Supervisor: Assoc. Prof. Dr. Müge Andaç Özdil
June 2020, 86 pages

A natural clay mineral, sepiolite ($Mg_4Si_6O_{15}(OH)_2 \cdot 6H_2O$), with a unit cell formula has fibrous structure, which has inside channels and sepiolite's high surface area lets inorganic and organic ions penetration into the clay structure. These properties make to be candidate for removing cationic molecules, heavy metals, organic compounds and even pesticides in industrial field. Polymer-based cryogels are known to be frequently used in purification and removal processes. In recent years, the use of sepiolite group of cryogels with composite materials and cryogels in water treatment systems has attracted attention. In this thesis, heavy metal (As, Pb, Cr, Cd etc.) removals from water environment with sepiolite embedded cryogels was investigated. The surface morphology and porosity of sepiolite embedded nanocomposite was characterized by Fourier Transform Infrared (FTIR), scanning electron microscopy (SEM), transmission electron microscopy (TEM), computed microtomography (mCT), puffing studies, flow and surface area evaluations. Binding tests will be performed by investigation of impact of initial concentration of a certified material. The impact of nanocrystallized sepiolite mineral on the amount of adsorbed metal from certified heavy metal solutions was determined using ICP-MS. Cryogels without sepiolite added were prepared as controls. This study demonstrates that the presence of

sepiolite increases the heavy metal adsorption. The sepiolite embedded nanocomposites were applied to a continuous treatment system for heavy metal removal from water solutions. Accordingly, %90 of heavy metals (Cr, Fe, Co, Zn and Cd) were adsorbed onto sepiolite embedded nanocomposite cryogels with maximum adsorption capacity. The adsorption time of sepiolite embedded nanocomposite cryogels was obtained as 30 minutes. Furthermore, the binding isotherms were evaluated by Langmuir and Freundlich models for heavy metals as Mn, Ni, As, Se, Cd, Sb and Co. It was calculated that Langmuir isotherm was well fitted with adsorption via monolayer. In addition, the binding mechanism of sepiolite embedded nanocomposite cryogels was defined by pseudo second order kinetics. It was concluded that adsorption mechanism of heavy metals onto sepiolite embedded nanocomposite cryogels can be explained by chemically controlled.

Keywords: Sepiolite, Nanocomposite cryogel, Heavy metal removal, Adsorption

ÖZET

SULARDAN AĞIR METAL ARITIMI İÇİN SEPİYOLİT İÇERİKLİ NANOKOMPOZİT KARTUŞLAR

Çağtay ÇİÇEK

Yüksek Lisans, Çevre Mühendisliği
Tez Danışmanı: Doç. Dr. Müge ANDAÇ ÖZDİL
Haziran 2020, 86 sayfa

Sepiyolit ($Mg_4Si_6O_{15}(OH)_2 \cdot 6H_2O$), yeryüzünde jeolojik süreçler sonucunda doğal yollarla oluşan ve kendine özgü nanometrik ölçekteki tüpsü kristal yapısı nedeniyle üstün sorptif, reolojik ve katalitik niteliklere sahip olan kil grubu bir fillosilikat mineralidir. Bu özellikleri ile sepiyolit endüstriyel bakımdan birçok alanda kullanılmaktadır. Son yıllarda, yüksek akış yolu özellikli makrogözenekli jel malzemelerin (kriyojellerin) ayırma ortamı olarak kullanılmasına yönelik çalışmalar oldukça önem kazanmıştır. Bu tez çalışması kapsamında, sulardaki ağır metallerin (As, Pb, Cr, Cd vb.) uzaklaştırılması amacıyla, farklı oranlarda sepiyolit içeren makrogözenekli kompozit kartuşlar hazırlanmıştır. Hazırlanan makrogözenekli nano-kompozit kartuşlar, taramalı elektron mikroskobu (SEM), fourier transform kızılötesi (FTIR) spektroskopisi, bilgisayarlı mikro tomografi (mCT), sepiyolit yükleme miktarı, jel oluşum verimi, akış dinamiği ve şişme deneyleri ile karakterize edilmiştir. Ağır metal uzaklaştırma etkinliği çalışmaları sürekli sistemde incelenmiştir. Buna göre, belirlenen ağır metallerin (Cr, Fe, Co, Zn ve Cd) %90'ı sepiyolit içerikli nanokompozit kriyojeller üzerine en yüksek kapasite ile adsorplanmışlardır. Sepiyolit içerikli nanokompozit kriyojellerin adsorpsiyon zamanı 30 dakika olarak belirlenmiştir. Dahası, Mn, Ni, As, Se, Cd,

Sb ve Co gibi ağır metallerin bağlanma izotermleri Langmuir ve Freundlich modelleri ile incelenmiştir. Yapılan hesaplamalar sonucunda Langmuir izotermi ile tek tabakalı adsorpsiyon modelinin örtüştüğü belirlenmiştir. Buna ek olarak, ağır metallerin bağlanma mekanizması için yalancı ikinci derece kinetik modelinin uyumlu olduğu gözlenmiştir. Buna bağlı olarak, bağlanma mekanizmasının kimyasal kontrollü olarak ilerlediği sonucuna varılmıştır.

Anahtar Kelimeler: Sepiyolit, Nanokompozit kriyojel, Ağır metal uzaklaştırılması, Adsorpsiyon.

ACKNOWLEDGEMENT

I would first like to thank my thesis advisor Assoc. Prof. Müge Andaç Özdil. The door to her office was always open whenever I ran into a trouble spot or had a question about my research or writing. She consistently allowed this paper to be my own work, but steered me in the right the direction whenever she thought I needed it.

I would also like to thank the experts who were involved in the validation survey for this master thesis: Assist. Gülgün Aylaz, PhD student. Without her passionate participation and input, the validation survey could not have been successfully conducted.

I would also like to acknowledge Prof. Adil Denizli for opening his laboratory for my experiments and always have been supportive, and helpfull attitude.

Finally, I must express my very profound gratitude to my parents and to my dear friend Ahsen N. Odabaşoğlu for providing me with unfailing support and continuous encouragement throughout my years of study and through the process of researching and writing this thesis. This accomplishment would not have been possible without them. Thank you.

This thesis study supported by Hacettepe Üniversitesi Bilimsel Araştırma Projeleri Koordinasyon Birimleri. Project Number: FYL-2018-17668.

Çağtay ÇİÇEK
June 2020, Ankara

INDEX

FIGURES INDEX

TABLES INDEX

SYMBOLS & ABBREVIATIONS

Symbols

Q	Adsorption Capacity
Ci	Initial Concentration
Cf	Final Concentration
m	Mass
V	Volume
OH-	Hydroxide
S_2	Sulfur
Sb	Antimony
Co	Cobalt
Mo	Molybdenum
Zn	Zinc
Cu	Copper
Cr	Chromium
Pb	Lead
Hg	Mercury
Fe	Iron
As	Arsenic
Cd	Cadmium
Ni	Nickel
CaO	Calcium Oxide
H_2S	Hydrogen Sulfide
SiO_2	Silicon Monoxide
Na_2O	Sodium Oxide
TiO_2	Titanium(II) Oxide
K_2O	Potassium Oxide
Fe_2O_3	Iron(III) Oxide
Al_2O_3	Aluminium Oxide
MgO	Magnesium Oxide
LOI	Loss On Ignition

HEMA	2-Hydroxyethyl Methacrylate
PEGDA	Poly Ethylene Glycol Diacrylate
TEMED	N,N,N,N-Tetra-Methylethylenediamine
APS	Ammonium Persulfate
HCl	Hydrogen Chloride
PHEMA	Poly 2-Hydroxyethyl Methacrylate

Abbreviations

GFAA	Graphite Furnace Atomic Absorption
FAAS	Flame Atomic Absorption
ASV	Anodic Stripping Voltammetry
AAS	Atomic Absorption Spectrophotometry
AES	Atomic Emissions Spectroscopy
XRF	X-ray Fluorescence
IDMS	Isotope Dilution Mass Spectrometry
EPXMA	Electron Probe X-ray Micro-analysis
DPASV	Differential Pulse Anodic Stripping Voltammetry
LAMMA	Laser Microprobe Mass Analysis
NPL	National Priorities List
HPLC	High-Performance Liquid Chromatography
ETAAS	Electrothermal Atomic Absorption Spectroscopy
PSA	Potentiometric Stripping Analysis
RNAA	Radio Chemical Neutron Activation Analysis
AFS	Atomic Fluorescence Spectrometry
PEUF	Polymer Enhanced Ultrafiltration
MEUF	Micellar Enhanced Ultrafiltration
EF	Electroflotation
EC	Electrocoagulation
ED	Electrodeposition
CNTs	Carbon Nanotubes
MWCNTs	Multi-walled
SWCNTs	Single-walled
EDCs	Endocrine Distruptive Compounds
FIB/SEM	Focussed Ion Beam Scanning Electron Microscopes

BET	Brunauer-Emmett-Teller Method
SEM	Scanning Electron Microscopy
SN	Sepiolite-Free
S8	Sepiolite-Containing
mCT	Computed Microtomography

1. INTRODUCTION

We are living in an industrializing world and growing industries has toxical consequences such as contamination of heavy metals in nature and especially in waters. Heavy metal exposure may cause many diseases, health problems, physcological problems and even deaths. In addition to that these diseases and problems last for very long years and exposure to heavy metals has very toxic effect on every living organism. Not only industries but some geological events may also cause heavy metal contamination such as weather events, abrasion and corrosion, volcanic eruptions [1][2][3][4].

Heavy metals are found in wastewater formed after industrial activities, garbage leakage waters and leaking from mining sites due to rain. This water mixture into the receptive environments, such as lakes, rivers, groundwater and accumulate in sediments. Consequently, pollution values even miles away from the discharge point protect without losing. Therefore, they protect pollution values without losing it, even miles away from the discharge point [5].

Heavy metals have toxic and carcinogenic effects and there is also a tendency to accumulate in live organisms. It is called bioaccumulation. Bioaccumulation means when chemical concentration in a biological organism meets his concentration in nature, it increased over the time. Compounds taken and stored into the body, faster than metabolized or excreted [6].

Heavy metals are metals relevant with contamination and toxicity or ecotoxicity; or It is defined as semi-metals. Nowadays, heavy metal has many definitions depending on their atomic weight and chemical features. Density of heavy metals is generally >5g/cm3. In medicine, the definition of heavy metal is regardless of the atomic weights of the elements, it is defined as all metals which has toxic effects [7][8].

Heavy metals are explained as important and unimportant according to their effect on biological processes. Those found in the components of vitamins and hormones are classified as vital. In addition to that, they show toxic effect after a certain concentration. In contrast to that, non-vital heavy metals have toxic effects from the initial concentrations, even at low concentrations, they can affect the human sanity and health problems [9].

But the main sources which are the contamination from heavy metals in wastewaters, are industrial ativities, mining processes and agriculturing. Exposing to heavy metals can cause also some deadly diseases like cancer, immune system failure, kidney failure, hearth attacks, etc. [10][11]. Because of these negative effects we need to remove them from our environment.

Heavy metal removal from aqueous samples has many diffrent methods, such as adsorption, electrochemical treatment technologies, chemical precipitation [12]. Adsorption is the main focus of this master thesis.

Cryogels are super-microporous gel network, which are produced under semi-frozen conditions [13]. Cryogels have three-dimensional hydrogen matrices and it helps us to incorporate sepiolite into cryogels. Cryogels are also usable for removal of heavy metal studies [14][15].

Cryogels are a good alternative material for heavy metal removal systems, due to their high hydrophilicity, swelling in water-insoluble, biocompatibility, flexibility and high mechanical stability properties. The poring material in cryogels is ice crystals, unlike many polymers that contain toxic organic compounds as pores [16].

Because of their physical, chemical and biologic properties; cryogels can be use in various sizes and shapes. In addition to that their pore size is also very useful for separating metal ions from water [17].

But there are not many heavy metal adsorption studies from water by using sepiolite embedded cryogels. Both cryogels and sepiolite have very high efficiency for removal studies. This thesis study shows that this nanocomposite cartridges are useful for removal of heavy metal from aqueous samples. In addition to that, they are cost-friendly and have high efficiency.

In this study, we used sepiolite embedded cryogels to adsorb heavy metals from aqueous solutions. Sepiolite has a lot of functional applications in cosmetics, agriculture, detergents, deodorants, etc. On the other hand, it has high efficiency for adsorbing heavy metals. Sepiolite is a clay mineral, which has the ability of adsorbs heavy metals, due its crystal structure. It has a stable chemical form and inexpensive clay mineral, which suits for the heavy metal removal by adding some chemical component for filter to heavy metal ions. Sepiolite embedded cryogels are very functional for adsorbing heavy metal ions [18][19][20].

This thesis study is composed of 4 chapters. First chapter contains general information and literature summary about thesis topic. Second chapter of the thesis contains data used, data source, data analysis and evaluation method. Third chapter of the study includes the results and evaluation section. Fourth chapter includes the general evaluations about the result of this study.

2.GENERAL INFORMATION

2.1. Heavy Metals

These elements occur on earth and very toxic to the human health and environment, there a lot of heavy metals in our habitat but the most known are copper, lead, arsenic, cadmium, mercury, iron, manganese, silver, zinc, selenium. The gravity of heavy metals is about 5 times the gravity of water [1].

These elements are naturally formed on the earth. Environmental pollution from these metals is generally caused by anthropological activities such as industrial activities, metal use in agriculture, mining and also weather events, abrasion and corrosion; volcanic eruptions are also among the factors that cause heavy metal pollution [1][2][3].

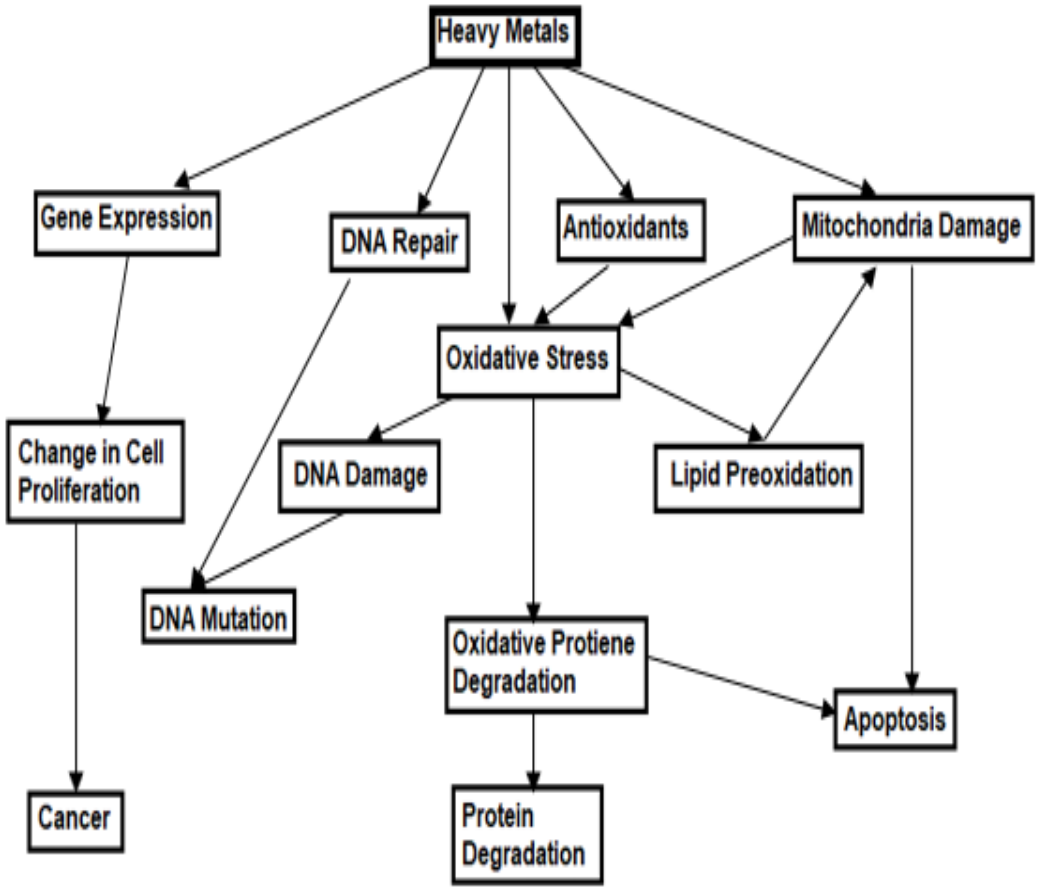

Figure 2.1. Intracellular effects of metals [21].

Exposure to heavy metals can give toxic on human body after a certain of concentrations (1-10 ppm) and even at low concentrations, they cause deterioration of psychological structure and cause health problems. But some of them are very toxic even at very low concentrations (0.001-0.1 ppm) such as mercury and cadmium [22].

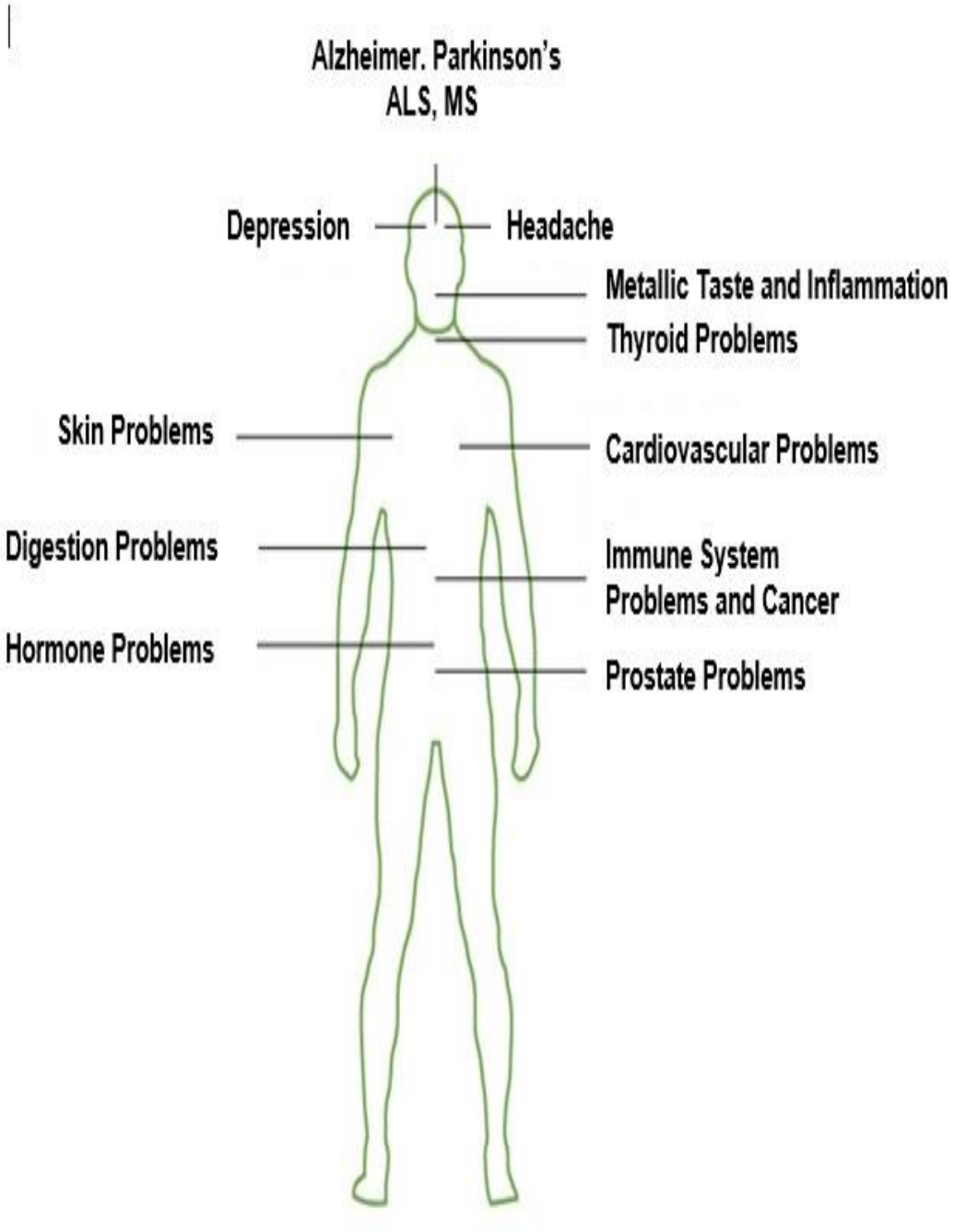

Figure 2.2. Symptoms due to heavy metals [23].

Heavy metal exposure can cause serious diseases which are alzheimer, parkinson's, depression, headache, metallic taste and inflammation in the mouth, thyroid problems, skin problems, digestion problems, hormone problems, cardiovascular problems, immune system problems, prostate problems and cancer. These health problems caused by heavy metals, need serious diagnoses and treatments but most of them have limited treatment options; consequently, this gives rise to high mortality rates. Mercury, lead, cadmium and copper are the leading metals with the most toxic effects [10][11].

Heavy metal quantities are in the soil usually ranges from 1-100,000 mg kg^{-1}. Heavy metals have negative effects on soil quality, product yield and because of it; this contamination deals great danger to every living being [24].

2.1.1. Copper (Cu)

Copper can be found in soil, water and atmosphere, also in animals and plants. It has a reddish color and is used for wires, pipes, cookware, cables, birth control pills, etc. It is also used in swimming pools and drinking waters in the form of copper sulfate. The lower exposer of copper has no harm to human body. But higher amount of it can cause diarrhea, headaches, dizziness, stomach cramps and nausea [25].

The huge amount of exposure to copper dust can cause brain, kidney or liver failure, which is called 'Wilson's diseases' [26].

Copper concentration in the air is about 200 ng/m^3. But at the area of smelters, this number raises to 5,000 ng/m^3. Because of that, people who lives near mining and smelter industries have very big risk to exposure copper by the air. Many people might be exposed to copper by the drinking water and concentration of it is 1,300 ppb, but in the tap water it is about in the range of 20-75 ppb. But, because of the dissolving of the copper from pipes of copper and the water waiting in the pipes, concentration of the copper can reach over 1,000 ppb. Because of the power plants exit water, algea control, etc. copper concentration in the lakes and rivers is up to 2800 ppb, but generally copper concentration in

the rivers and lakes is in the range of 0.5-1,000 ppb. If we examine the soil, natural copper concentration is in the range of 2-250 ppb. Owing to minnings, copper industries and sewage treatment plants; copper concentration in the soil can rise to 17,000 ppb [25].

2.1.2. Lead (Pb)

This heavy metal naturally occurs in atmosphere and oceans. It can be found in industrial sources, such as batteries, toys, gasoline, pipes, house paints, bullets, vehicle exhausts, etc. and also in cigarettes, foods, drinking water and domestic sources. The most important lead exposure caused by drinking water and foods [27][28].

Exposure to lead in a long term can cause fetal brain damage, kidney diseases, circulatory and nervous system diseases [29].

Detecting lead from waters, sediments, soils and dusts; the most common and known methods are AAS, Atomic Emissions Spectroscopy (AES), X-ray Fluorescence (XRF), ASV, Isotope Dilution Mass Spectrometry (IDMS) [30].

Table 2.1. Quantitiy of lead in soil, water and air [31].

Medium	Median[a]	Geometric Mean[a]	Geometric Standard Deviation	NPL
Water	0.118 ppb	0.0075 ppb	13.8 ppb	657 ppb
Soil	1.11 ppb	878 ppb	19.8 ppb	655 ppb
Air	0.00165 ppbv	0.0025 ppbv	32.6 ppbv	50 ppbv

2.1.3. Arsenic (As)

Arsenic has no good effects on humans. It is highly toxic and cause several damages on human body when exposed to it. Arsenic naturally occurs in waters, some insecticides and fossil fuel combustions [27].

It can also be found in industrial activities and the soil. Arsenic exposures can cause muscle cramps, burning of throat and mouth, anorexia and vomiting. Huge amount of arsenic in the human body can cause liver and skin cancer [32].

There are several methods for detecting arsenic such as ICP/MS, ICP/AES, AAS, Colorimetric Photometry, XRF and GFAAS. Arsenic concentration in the soils is in the range of 3-4 ppm, but in the contamined areas, which are mining and industrial areas, may have higher concentration of arsenic. Concentration of arsenic in groundwater and surface water is about 1 ppb, but in the contaminated ares, it may rise to 1,000 ppb. In the air, arsenic concentration is in the range of 1-2,000 ng/m^3 [33].

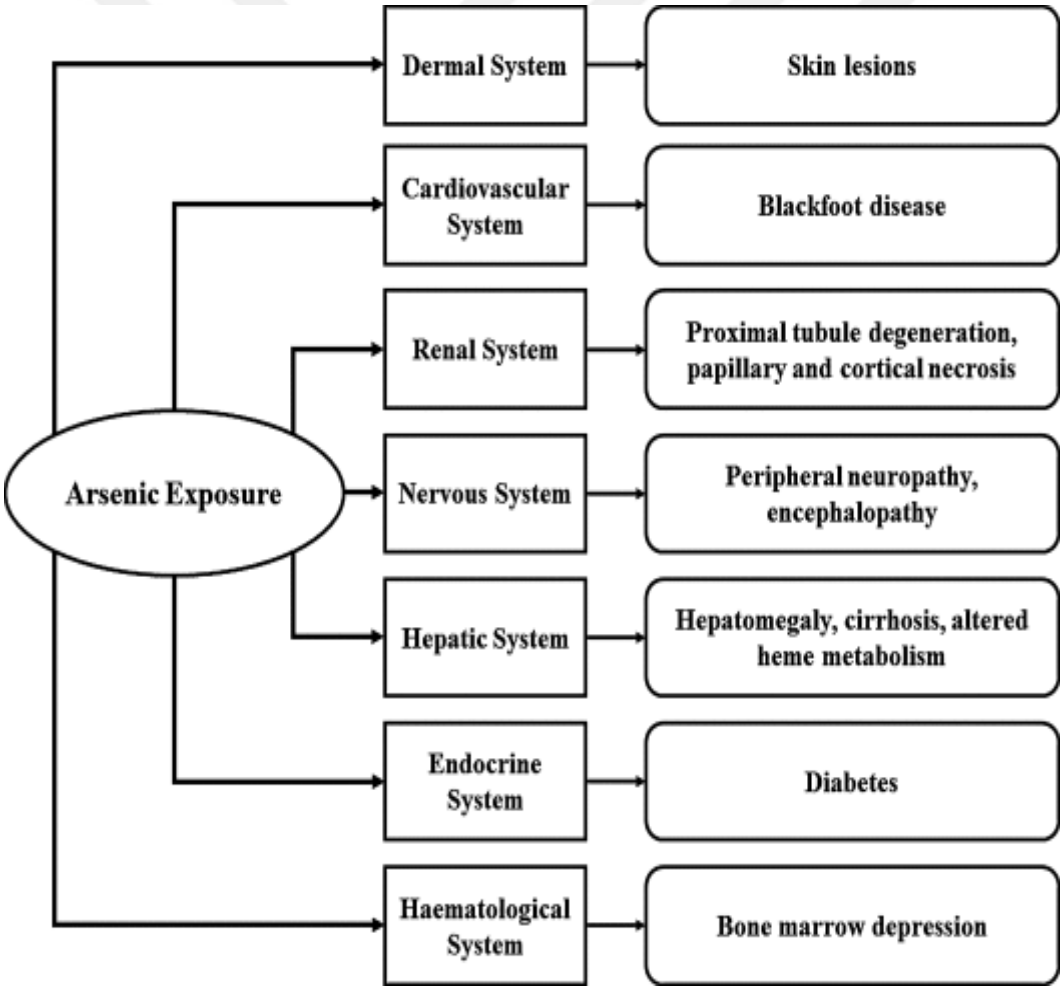

Figure 2.3. Health problems caused by exposure to arsenic [34].

2.1.4. Cadmium (Cd)

This heavy metal is mostly found in soils, sediments, air and seawater. Cadmium compounds, using by mines and industries to process plastics, batteries, alloys and pigments [35].

The largest source of cadmium is from tobaccos. It contains huge quantity of metals [36]. Emitted cadmium from the industries into fertilizers, groundwater and sewage which can be taken up by plants. Because of that, many people expose to cadmium by the foods; such as fruits, grains, vegetables and cereals [37][38].

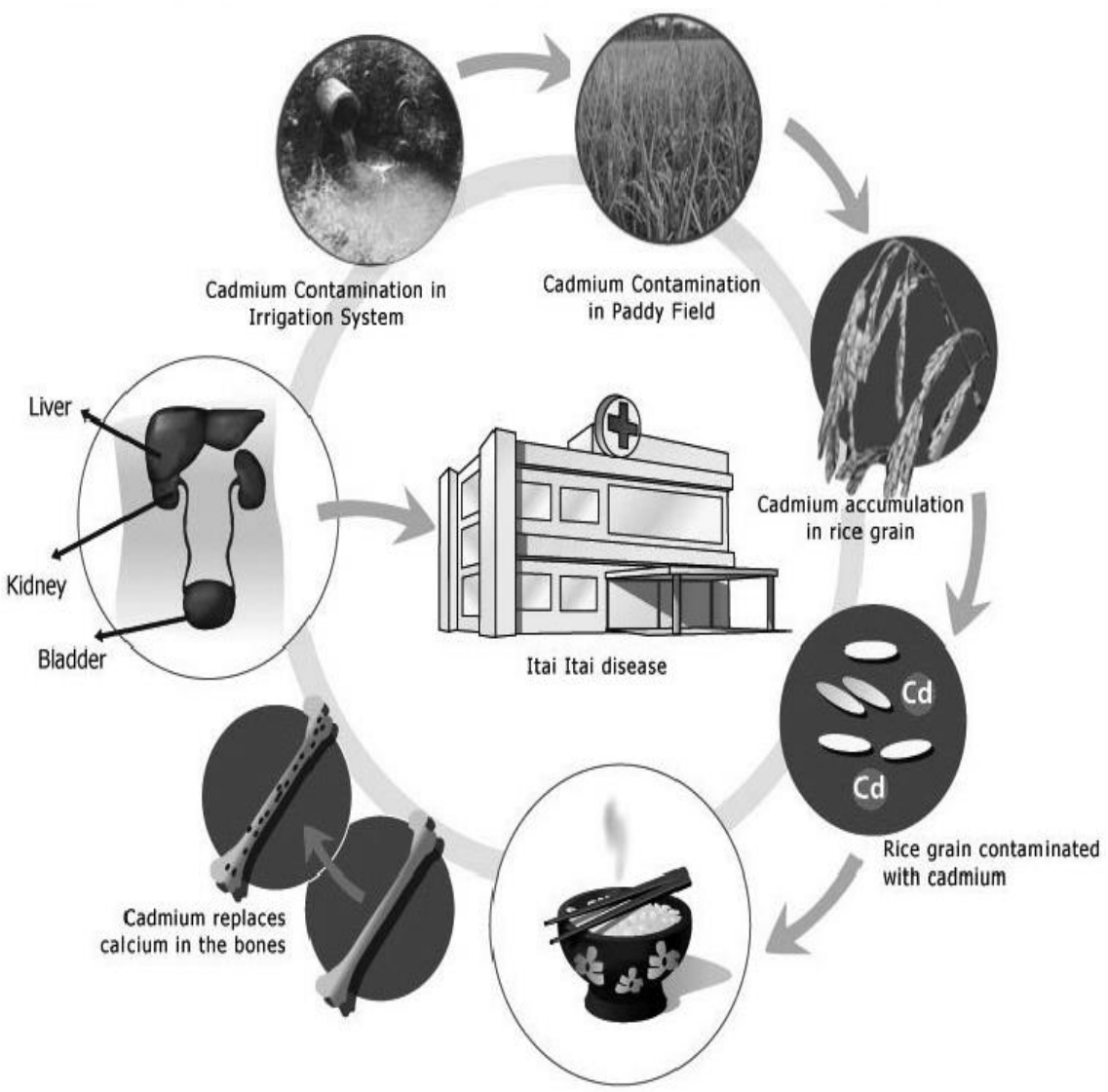

Figure 2.4. Cadmium's health effects on human body [39].

Exposing to cadmium can cause lungs damage and lung cancer, kidney disease, vomiting, diarrhea, fragile bones, anemia, liver diseases and nerve or brain damages. Concentration of cadmium in the air is showing differences because of the region characteristics. According to that, cadmium concentration in pastoral regions is between the number values of 0.1-5 ng/m^3, in urban regions is in the range of 2-15 ng/m^3, in industrial regions is in the range of 15-150 ng/m^3. Concentrations of cadmium minimum and maximum rates in the ocean are 5-110 ng/L, in the groundwater and surface water are generally <1 µg/L. Cadmium in the soils at a concentration of 0.06-1.1 mg/kg. Some of the detection methods for cadmium are AAS, GFAAS, ICP/MS, ICP/AES, XRF, NAA, Potentiometric Stripping Analysis (PSA) and Radio Chemical Neutron Activation Analysis (RNAA) [40].

2.1.5. Mercury (Hg)

Mercury has a silver color and it looks like shiny metal. It is generally used for thermometers, batteries, dental amalgams, automotive, building industries, chemicals, metal processing and electrical equipments [41].

Mercury is very toxic heavy metal for the environment and human health. Most of the exposures to mercury based on high consumption of seafood and contaminated fish [42].

Exposure to mercury can cause Rheumatoid arthritis, brain damages, kidney diseases and circulatory system diseases [29].

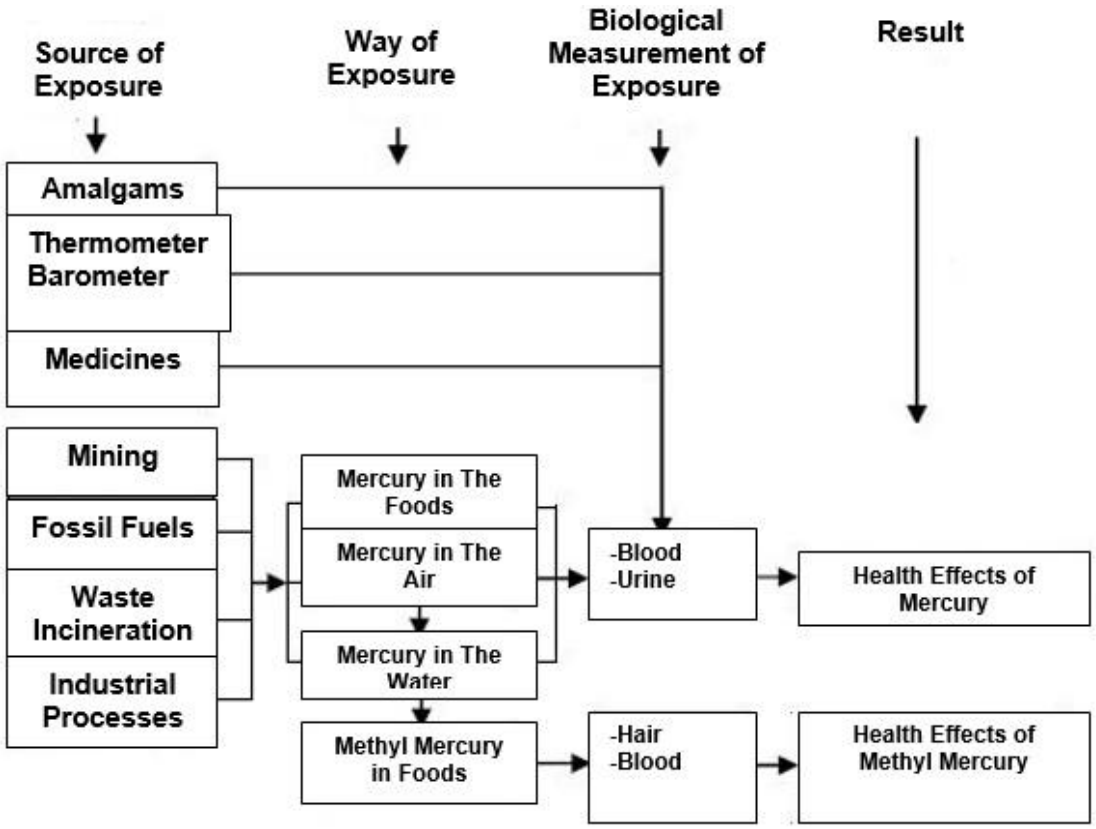

Figure 2.5. Mercury exposure chart [43].

Mercury concentration in the air is in the range of 10-20 ng/m^3, this numbers rise up in the contaminated areas. The unpolluted waters generally have less than 5 ng/L concentration of mercury; but in the rain waters and fresh snow, mercury concentration is about 200 ng/L. Mercury concentration in the soil is in the range of 20-625 ng/g. There are several methods to measure and detect the mercury such as ETAAS, ICP/AES, ICP/MS, NAA, Anodic Stripping Voltammetry (ASV), Atomic Fluorescence Spectrometry (AFS) and XRF [44].

2.2. Heavy Metal Removal Methods from Water Solutions

As known, heavy metals are very toxic even at the lowest concentrations (0.001-0.1 ppm). Therefore, they had to be cleaned from the soil, water and air. Heavy metals have some natrural (water) sources, such as erosions, volcanic eruptions and explosions, activities of weather, living creature's activities, and also anthropogenic activities, such as agricultural activities, industrial activities, mining, fuel combustion, sewage and landfills [45].

There are many removals of heavy metal methods from aqueous samples and the most commons are chemical precipitation, ion-exchange, membrane filtration, electrochemical treatment technologies, adsorption [12].

2.2.1. Chemical Precipitation Methods

This is a simple and mostly cheap method. It can be removed from aqueous samples by OH^- and S^{2-} precipitation [12]. As this method is cheap and easy to apply, it is one of the most used methods. In this method, adsorption efficiency at large range concentrations are considerably high.

In studies, CaO and H_2S are used for Zn, Cu and Pb ions elimination, the removal success is more than 90 percentage in all of them. In addition to that, when CaO and MgO are used in Cr ions removal, the removal efficiency has reached 99 percentage (Table 2.2). Other studies can be examined in Table 2.2.

Table 2.2. Chemical precipitation studies.

Heavy Metals	Heavy Metal Removal Methods		Heavy Metal Concentrations		Removal Success(%)		Research Groups	Ref.
Zn(II)	CaO	H_2S	32 mg/L	1.34 mM	99-99.3	94	Ghosh et al.	[46]
Cu(II)	CaO	H_2S	100 mg/L	0.018 mM	99.37-99.6	100	Chen et al., Alvarez et al.	[47] [48]
Cr(III)	CaO, MgO		5363 mg/L		99		Guo et al.	[49]
Pb(II)	CaO	H_2S	100 mg/L	2.3 mM	99.37-99.6	92	Chen et al., Alvarez et al.	[47] [48]
Hg(II)	1.3-benzenediamido ethanethiolate		188 µg/L		99.9		Blue et al.	[50]

2.2.2. Ion Exchange Methods

Because of removal efficiency and treatment capacity, this method has been widely used for removing heavy metals from waters [51].

This method is based on ion exchange between ion exchanger solid phase and liquid phase. Heavy metals in water samples are replaced by cations in ion exchangers.

Table 2.3. Ion exchange studies.

Heavy Metals	Heavy Metal Removal Methods	Heavy Metal Concentrations	Removal Success (%)	Research Groups	Ref.
Zn(II)	Batch Experiments	65.4-654 mg/L	100	Athanasiadis et al.	[52]
Ni(II)	Batch Experiments	25 mg/L	93.6	Argun	[53]
Pb(II)	Batch Experiments	1036 mg/L	55	Inglezakis et al.	[54]

As can be examined from Table 2.3, different studies have been applied for removal Zn, Ni and Pb ions. While removal of Zn and Ni ions have high efficiencies, removal of Pb ions have relatively low compared to the others (Table 2.3).

2.2.3. Membrane Filtration Methods

There are some membrane filtrations methods, which are using for remove metals from water, such as 1) osmosis, 2) ultrafiltration, 3) electrodialysis and 4) nanofiltration [55].

2.2.3.1. Reverse Osmosis Membranes

This membrane holds the contaminant particles and let it pass to purified water. Reverse osmosis is very useful for salt purification from seawater, therefore it has a very big amount of usage [56].

Considering the studies, this method is one of the most important method due to its high removal success for heavy metal removal. When examined the studies of RO, removing As ions from water solutions have more than 91%, removing Zn ions from water solutions have 98.9%, removing Ni ions from water solutions

have 99.3%, removing Cu ions from water solutions have 99.5% efficiencies (Table 2.4).

Table 2.4. Reverse osmosis studies.

Heavy Metals	Heavy Metal Removal Methods	Heavy Metal Concentrations	Removal Success(%)	Research Groups	Ref.
As(I)	Reverse Osmosis	<500 mg/L	91-99	Chan et al.	[57]
Zn(II)	Reverse Osmosis	64-170 mg/L	98.9	Ipek	[58]
Ni(II)	Reverse Osmosis	44-169 mg/L	99.3	Ipek	[58]
Cu(II)	Reverse Osmosis	500 mg/L	99.5	Mohsen et al.	[59]

2.2.3.2. Ultrafiltration Membranes

This membrane technique is used to remove colloidal and dissolved materials. There are two ultrafiltration methods, first one is polymer enhanced ultrafiltration, and the other one is micellar enhanced ultrafiltration. PEUF is applied for eleminate of heavy metals from aqueous samples. PEUF is using water soluble polymers for metal ions. MEUF is also applied for separate metals from wastewater. It depends on surfactants for wastewater [12].

Table 2.5. Ultrafiltration studies of membranes.

Heavy Metals	Methods	Membrane		Heavy Metal Con.		Removal Success (%)		Research Groups		Ref.
Cu(II)	PEUF	Polyethersulfone	Ceramic	50 mg/L	160 mg/L	94	99.5	Molinari et al.	Camarilloa et al.	[60] [61]
Ni(II)	PEUF	Polyethersulfone	Polycarbonate	50 mg/L	0.2 mM	100	98.6	Molinari et al.	Danisa et al.	[60] [62]
Cr(III)	PEUF	Polyethersulfone		10 mg/L		99.5		Barakat et al.		[63]
Cd(II)	MEUF	Polysulfone	Amicon regenerated cellulose	50 mg/L	0.5 mM	92	99	Huang et al.	Landaburu-Aguirre et al.	[64] [65]
Zn(II)	MEUF	Polysulfone	Amicon regenerated cellulose	51 mg/L	0.5 mM	98	99	Huang et al.	Landaburu-Aguirre et al.	[64] [65]
Pb(II)	MEUF	Ceramic		4.4 mg/L		99		Ferella et al.		[66]

As seen in Table 2.5, Cu ions removal was achieved with polyethersulfone membrane and ceramic memrane. Ceramic membrane also used for remove Pb ions from water solutions. More than 90 percent removal efficiency has been achieved with these two membranes. Polyethersulfone membrane also used for Ni and Cr ions removal, the results are the same as high as Cu ions removal. Polysulfone and amicon regenerated cellulose membranes are used for remove Cd and Zn ions from water solutions, and this study achieved very high efficiency numbers.

2.2.3.3. Electrodialysis Membranes

This membrane's method is using electrical force for separating metal ions from water. Electrodialysis is simply using exchange of anionic and cationic ions to produce drinking water, salt from seawater, lakes and some industrial treatments [67].

Table 2.6. Electrodialysis studies of membranes.

Heavy Metals	Heavy Metal Removal Methods	Heavy Metal Cons.	Energy Consumption	Removal Success (%)	Research Groups	Ref.
Cr(IV)	Electrodialysis	20 mg/L	50 V	94.45	Nataraj et al.	[68]
Cu(II)	Electrodialysis	4000 mg/L	562.08 kWh/m^3	88.75	Caprarescu et al.	[69]

The studies of heavy metal removal with electrodialysis from water solutions show high efficiencies. In Table 2.6, removal of Cr has 95% removal success, removal of Cu has 89% removal success. Based on these datas, this membrane is more effective at low concentrations.

2.2.3.4. Nanofiltration Membranes

Nanofiltration is cheaper than the reverse osmosis method and has a higher flow degree. It is a method that used for water and wastewater treatments. Nanofiltration method has very good efficiency for eleminate metal ions from aqueous samples [70].

In Table 2.7 shows us NF membrane's efficiencies depend on metal ion's concentrations. As instance this membrane has very high removal success for eleminate of Cr, Ni and As ions from aqueous samples. But the removal of Cr ions has maximum %66 removal efficiency.

Table 2.7. Nanofiltration studies of membranes.

Heavy Metals	Heavy Metal Removal Methods	Heavy Metal Concentrations	Removal Success(%)	Research Groups	Ref.
Cr(IV)	Nanofiltration	0.47 M	96-98	Tanninen et al.	[71]
Cu(II)	Nanofiltration	10 mM	47-66	Chaabane et al.	[72]
As(I)	Nanofiltration	100 ppb	>97	Figoli et al.	[73]
Ni(II)	Nanofiltration	5-250 mg/L	92-98	Murthy et al.	[74]

2.2.4. Electrochemical Treatment Technologies

This method's purpose is giving the water cation or anion ions and separating heavy metal ions through the electricity. Due to its electrical power, electrochemical treatments need to big amount of investments, therefore it does not have a widely usage. Some of the treatments are electroflotation (EF), electrocoagulation (EC) and electrodeposition (ED). Electroflotation (EF) can be use in liquid and solid contaminations and by the help of electrolysis, it can separate the floating ions on the wastewater surface. Electrocoagulation (EC) is using the electrical flow for floating to ions and separate them from the wastewater surface. It is used in industrial treatments [12].

Electrodeposition (ED) is electroplating metal ions to conductive surfaces, because of this, it prevents the corrosions and abrasions [75].

As we can examine in Table 2.8, some heavy metal ions removed from water samples with very high efficiency at the range of 2-110 mg/L. Such as; Cu, Zn, Ni, As, Mn. But Cr ions removal showed a hundred percentage yield even at high concentration.

Table 2.8. Electrochemical treatment studies.

Heavy Metals	Heavy Metal Removal Methods	Heavy Metal Concentrations	Removal Success (%)	Research Groups	Ref.
Cu(II)	Electroflotation	100 mg/L	98-99	Khelifa et al.	[76]
Zn(II)	Electroflotation	20 mg/L	96	Casqueira et al.	[77]
Ni(II)	Electroflotation	100 mg/L	98-99	Khelifa et al.	[76]
Cr(VI)	Electrocoagulation	1470 mg/L	100	Ölmez	[78]
As(I)	Electrocoagulation	2.24 mg/L	99	Parga et al.	[79]
Mn(II)	Electrocoagulation	100 mg/L	78.2	Shafaei et al.	[80]
Cu(II)	Electrodeposition	110 mg/L	90.4	Chang et al.	[81]

2.2.5. Adsorbents

2.2.5.1. Activated Carbon Adsorbents

Activated carbons have spacious mesopore and micropore capacity, internal surface area, and also, they are very useful for heavy metal removal. It is generally produced by heating processes and chemical processes [82].

Table 2.9. Activated carbon studies.

Heavy Metals	Heavy Metal Removal Methods	Capacity of Adsorptions	Removal Success (%)	Research Groups	Ref.
Cd(II)	Activated Carbon	9.01-24.83 mg/g	68	Obregón-Valencia et al.	[83]
Zn(II)	Activated Carbon	4.61 mg/g	98	Galiatsatou et al.	[84]
Pb(II)	Activated Carbon	148.77 mg/g	100	Bohli et al.	[85]
Cu(II)	Activated Carbon	17.78 mg/g	62	Bohli et al.	[85]
Ni(II)	Activated Carbon	24.07 mg/g	78	Bohli et al.	[85]

The only obstacle to their widespread use is they are relatively expensive. For this reason, it is widely researched that, their cheaper versions and performances remove various pollutants.

When Table 2.9 is examined, this membrane has the highest removal success in removing Zn and Pb ions from water solutions. But removal of Cd ions has 68% efficiency. But removal of Cu ions has 62% efficiency and removal of Ni ions have 78% efficiency.

2.2.5.2. Carbon Nanotubes Adsorbents

Carbon Nanotubes (CNTs) can use their thermal and chemical features with high efficiencies. There are two types of CNTs due to their layers, which are multi-walled (MWCNTs) and single walled (SWCNTs) [86].

Table 2.10. Carbon nanotube studies.

Heavy Metals	Heavy Metal Removal Methods	Heavy Metal Concentrations	Removal Success (%)	Research Groups	Ref.
Cu(II)	SWCNTs	10 mg/L	94	Sadeghinya et al.	[87]
Hg(I)	SWCNTs	0.1 µg/L	100	Globabaei et al.	[88]
Cu(II)	MWCNTs	2.38 mg/L	100	Oliveira	[89]
Zn(II)	MWCNTs	3.43 mg/L	81	Oliveira	[89]
Ni(II)	MWCNTs	3.74 mg/L	76	Oliveira	[89]
Pb(II)	MWCNTs	11.26 mg/L	97	Oliveira	[89]

In Table 2.10, MWCNTs and SWCNTs membranes have very high removal success for adsorbing heavy metals from water solutions. As a best example of this is Hg and Cu. These ions removed from water solutions with 100% efficiency. Pb ions removed with 97% efficiency at 11 mg/L and removal of Cu ions have

also high efficiency, such as 94% at 10 mg/L. Zn and Ni ions also removed with successable rate.

2.2.5.3. Biosorption

Biosorption is a biological adsorption and it is using for eleminate of metals from water samples. Biological polymers, industrial and agricultural wastes, microorganisms, plants can be used as biosorption [90].

Biosorption is removing metal ions from aqueous by biomass. Biosorption of metals generally depends on adsorption and ion replacement events.

Table 2.11. Biosorption studies.

Heavy Metals	Heavy Metal Removal Methods	Heavy Metal Concentrations	Removal Success (%)	Research Groups	Ref.
Cd(II)	Biosorption (Hypnea Valentiae)	25 mg/L	86.8	Rathinam et al.	[91]
Cu(II)	Biosorption (Cashew Nut Shell)	10 mg/L	86.03	SenthilKumar et al.	[92]

As we can examine in Table 2.11, studies carried with two types of biosorptions. Hypne Valentiae applied for removing Cd ions from water samples and it has %87 efficiency at 25 mg/L.

Cashew nut shell applied for removing Cu ions from water samples with %86 at 10 mg/L. Both of these removal methods have very high removal success.

2.2.5.4. Coagulation and flocculation

Coagulation is converting the dissolved pollutants in the wastewater into chemical collapsible flocs [93].

At the end of mixing wastewater at constant speed, small particles occured by the process of coagulation, that is the process of creating flocs that can collapse easily, which is the definition of flocculation [94].

Table 2.12. Coagulation and flocculation studies.

Heavy Metals	Heavy Metal Removal Methods	Heavy Metal Concentrations	Removal Success (%)	Research Groups	Ref.
Pb(II)	Coagulation and flocculation	7 mg/L	99	Pang et al.	[95]
Fe(III)	Coagulation and flocculation	5 mg/L	99	Pang et al.	[95]
Zn(II)	Coagulation and flocculation	5 mg/L	93.2	Pang et al.	[95]

In Table 2.12, as a result of these methods, extraordinary results were obtained in heavy metal removal. Pb and Fe ions removed from water samples with 99% efficiency which is very high. And removal Zn ions have also very high results and they removed with 93% efficiency.

2.3. Sepiolite

Sepiolite ($Mg_4Si_6O_{15}(OH)_2 \cdot 6H_2O$) is a phyllosilicate mineral of clay group, which occurs naturally as a result of geological processes on the earth and has superior sorptive, rheological and catalytic properties due to its unique crystalline tubular structure [18].

When the written sources are examined, it is seen that sepiolite has been known since 1809. Cronstedt named the sepiolite in his book as ‘Keffekil Tartarorum’ [96][97]. But Werner named it ‘Meerschaum’, which is mean sea foam, in 1809 [98][99]. However, the name sepiolite was officially given by Glocker in 1847 and he named it ‘Sepiolithus’. Sepiolithus is derived from squid fish in Greek [100][101].

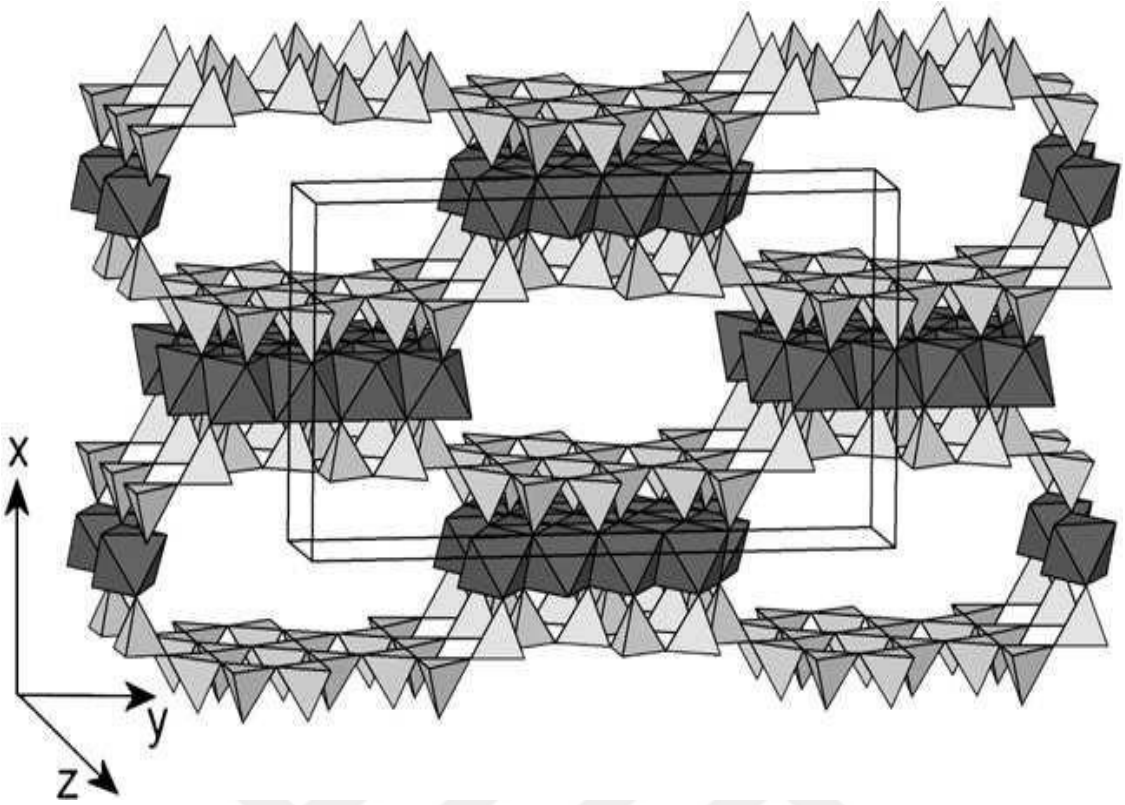

Figure 2.6. Crystal form of sepiolite [19].

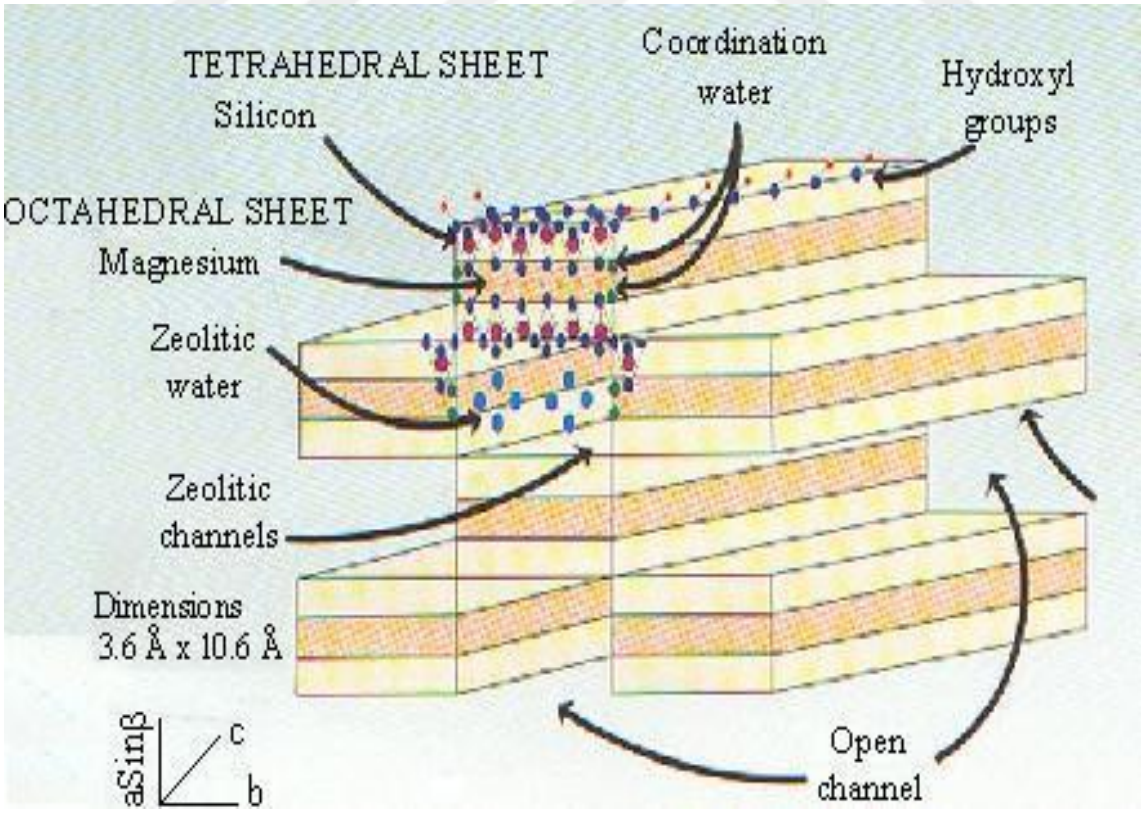

Figure 2.7. Scheme of fibre morphology in sepiolite [102].

Due to the chemical properties of the sepiolite crystal, it can keep heavy metals at the end of adsorption or cation exchange reactions. Chemically stable, inexpensive and suitable for surface modification are the most distinctive features of sepiolite in combination with different chemical components for various filtering purposes. Sepiolite with these characteristics are used in many areas of industrial maintenance and also Turkey has one of the world's largest sepiolite reserves [18].

Table 2.13. Chemical compositon of sepiolite [18].

Chemical Composition of Sepiolite	
Compounds	Weight (%)
Na_2O	0.25
TiO_2	0.30
K_2O	0.75
Fe_2O_3	1.92
CaO	3.26
Al_2O_3	4.17
MgO	15.17
SiO_2	52.76
LOI	21.42

2.3.1. Applications of Sepiolite

Sepiolite has been used for eleminate of metals from aqueous samples. Beacuse of the acid soaking methods, sepiolite can adsorb heavy metals in its pores [19]. Because of its porosity, surface area and sorption capacity, sepiolite can be used in various applications [103].

Sepiolite with some suitable pretreatments has been functional in downstream applications; environmental deodorants, absorbents, carriers, catalysts, paints, polyesters, NCR paper, pharmaceutical treatments, agents of decolorizing,

agents of anti-caking, rubbers, carriers of phytosanitary, cigaret filters, plastisols, filter aids, animal nutritions, detergents (dirt removal processes), cosmetics (jewelry production etc.), agriculture, grease thickeners, coatings of asphalt and drilling fluids [20].

Table 2.14. Sepiolite studies.

Application Method	Applied Operation	Research Groups	Ref.
Heavy metal removal with sepiolite	Acid soaking and High temperature calcination	Wang et al.	[104]
DNA transfer with sepiolite	Adsorption of DNA onto sepiolite	Smirnoc et al.	[105]
Adsorption of heavy metal with sepiolite	Functionalization of sepiolite with MPS	Celis et al.	[106]
Adsorption of chitosan on sepiolite	Electrostatic interplay in acidic environment	Darder et al.	[107]
Heavy metal removal with sepiolite	Sepiolite modification with trimethoxysilane	Doğan et al.	[103]
PLA and PCL nanocomposite preparation	Melt mixing sepiolite and montmorillonite	Fukushima et al.	[108]

In Table 2.14, sepiolite application methods are given. Most of these methods have been used in adsorbing heavy metals and the others applied in medicine and other fields by using sepiolite. Such as DNA transfer, chitosan adsorption and PLA-PCL preparation.

2.4. Cryogel

Cryogels are super-microporous gel networks developed by cryogelling of compound monomers or polymeric precursors at temperatures which are generally below zero [109].

Synthesizing cryogels must happen under semi-frozen situations and ice crystals function like porogens and pores, which are acting like a connecting of network,

are in the range of 20-100 μm, following the melting of ice crystals. After thawing crystals of ice, took a form like network of polymer and porogen of connected pores [13].

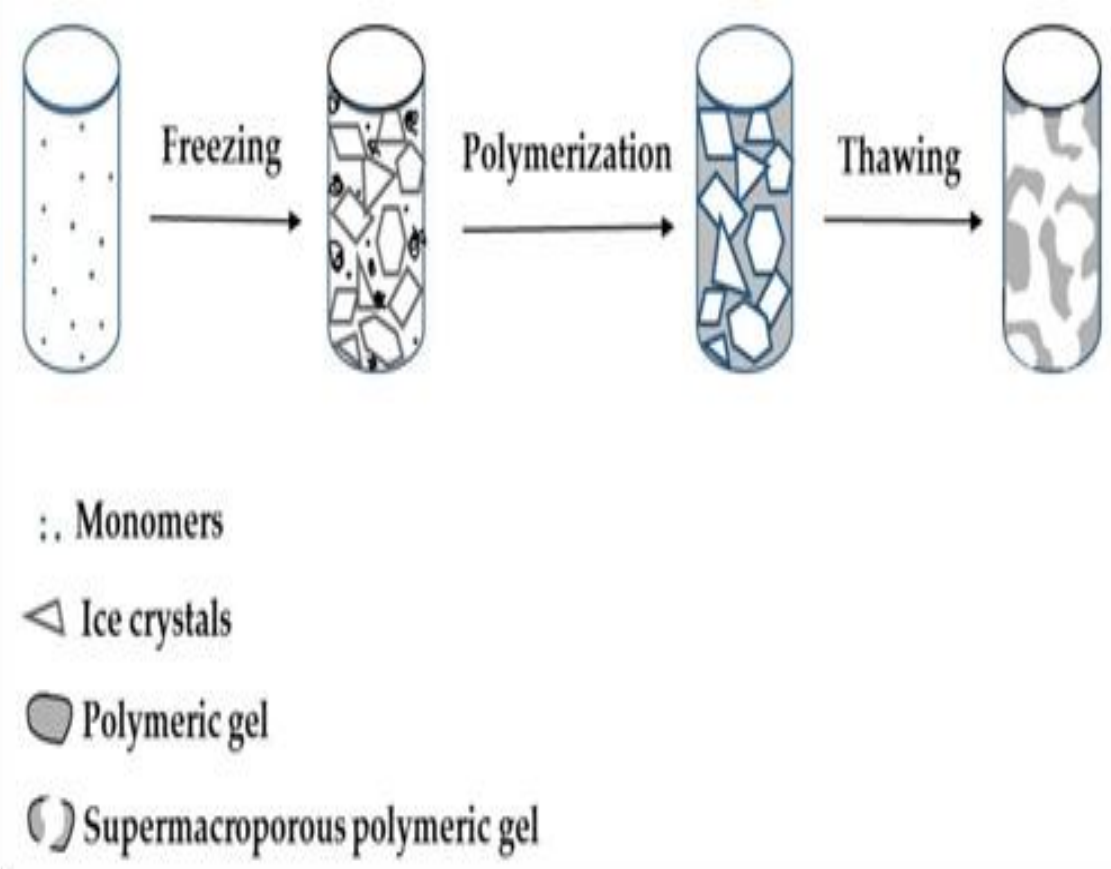

Figure 2.8. Supermacroporous cryogel preparation [110].

Cryogels have hydrogel matrices, which are three dimensional, they are synthesized by systems of indicator and activator under semi-frozen conditions. Cryogel characteristics are splendid due to their pore size, which is up to 100 μm. This gelation structure is compulsory for processes of purification and separation due to their mechanic strength, biocompatibility, flexibility and diffusion paths (which are very short). Cryogel preparation is very easy and reasonably priced, because of that, after the use of cryogels, they can be thrown away to prevent the possibility of contamination [111].

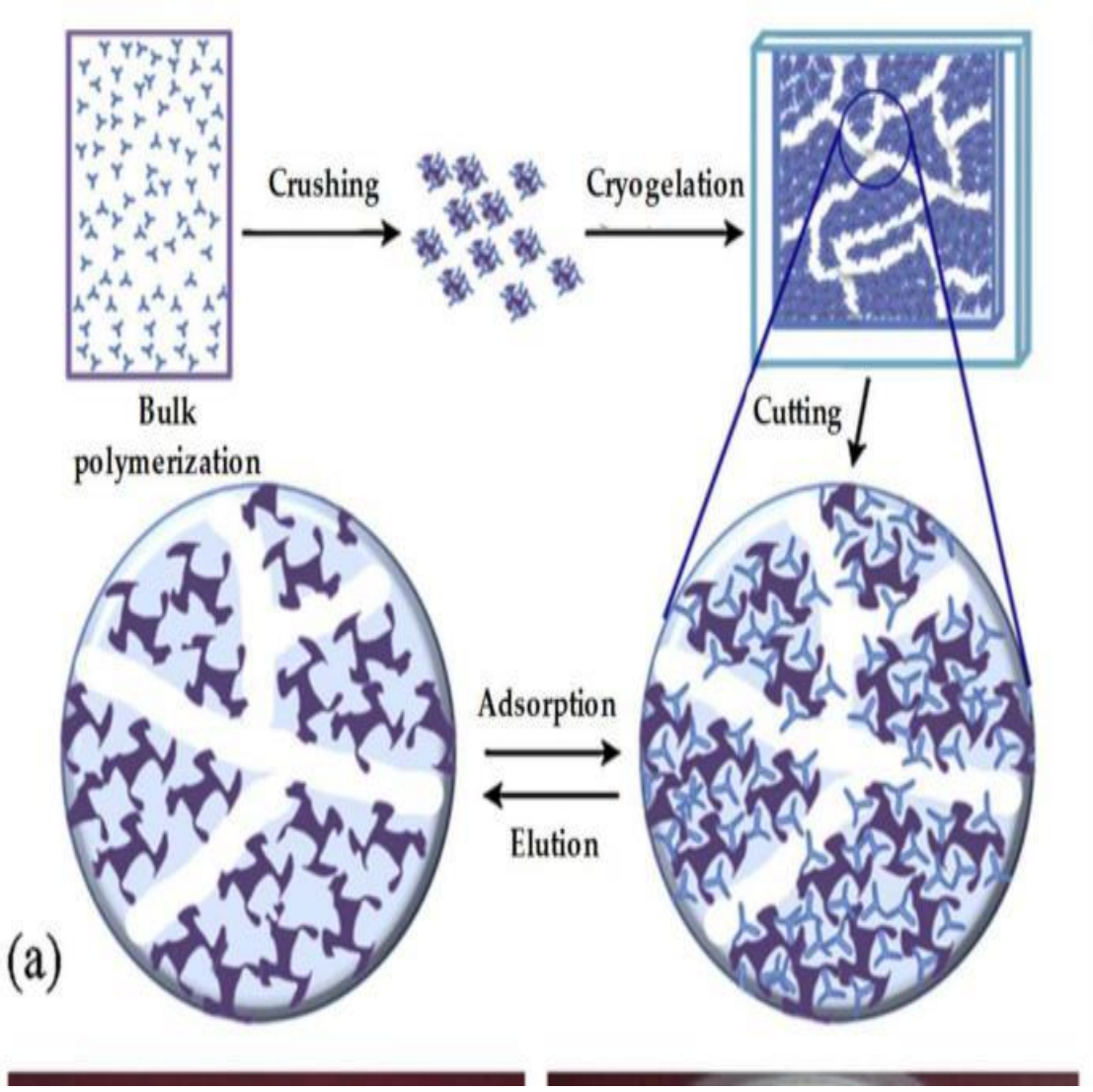

Figure 2.9. Composite cryogels [112].

Gel solution compounds, temperature, time of held and freezing degree of gelation, crosslinking type and degree are the basic agents that specify the characteristics of cryogel. In addition to that factors, pore size of cryogels are also very important due to biomedical applications of cryogels [113][114].

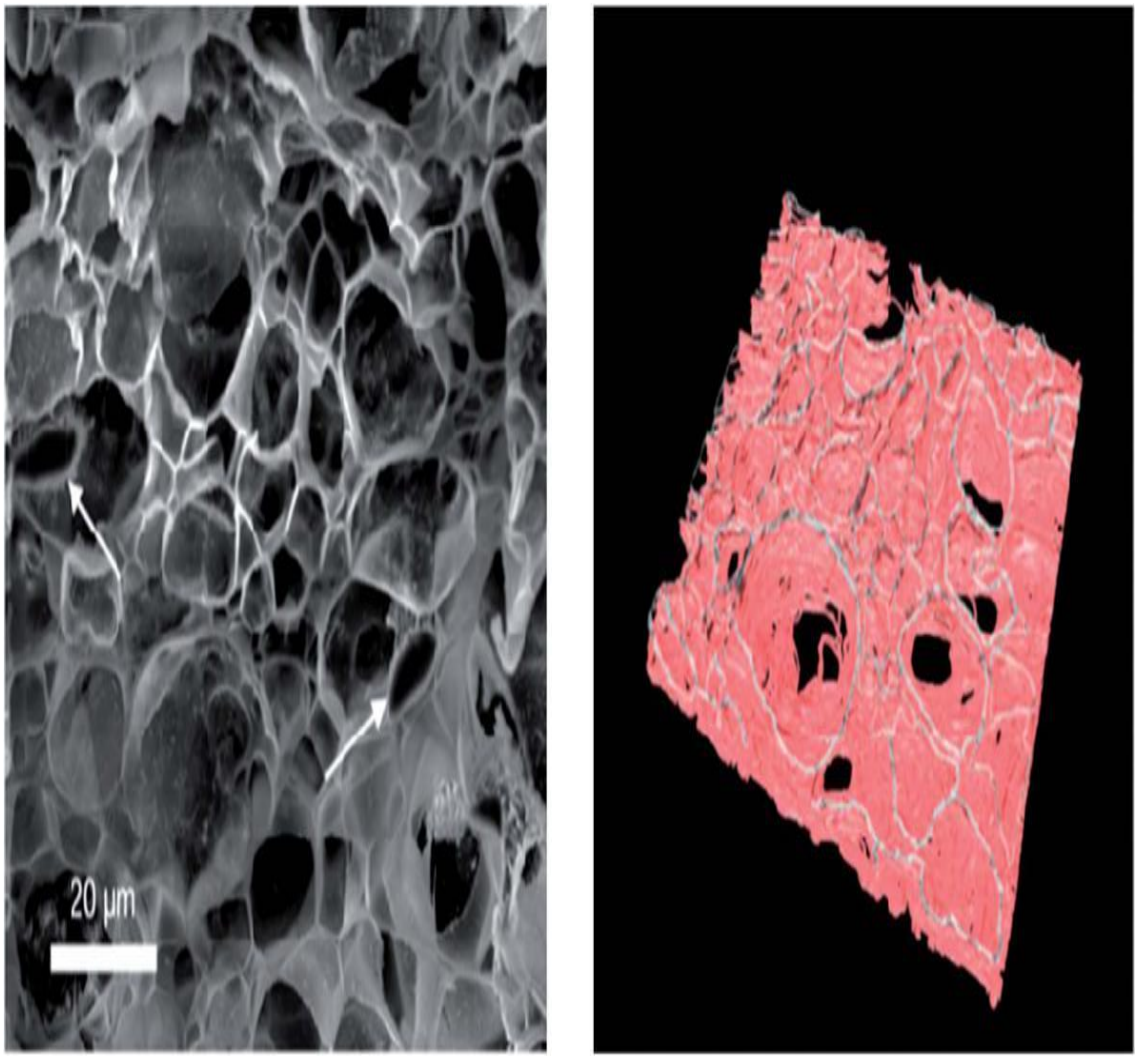

Figure 2.10. Left side is cryogel imaged by FIB/SEM (Arrow pointed to the cells)/Right side is 3D print of rebuild cryogel [115].

It was confirmed if the temperature is lowered, smaller pores can be form in the cryogelation studies. And also, the solvent crystallized faster to form smaller and more solvent crystals, because of that, denser and thinner pore walls are occurred [114][116].

2.4.1. Applications of Cryogel

Cryogels are used in many applications due to their hydrophobic polymer form, which quickly combines mechanical properties. Furthermore, they have elasticity, wide pore structure, short diffusion time, degradability, biocompatibility, nontoxicity, short retention time for both desorption and adsorption [14].

Some of the applications of cryogels are; heavy metal removal from environmental samples, scaffolds, bacterial disinfection, energy storage, bioreactor, target molecule capturing, phenol degradation, cell separation, tissue engineering, immobilization of biomolecules, controlled drug delivery, oil removal (from water), separator for organic pollutants, enzyme immobilization, affinity purification, endocrine disruptive compounds (EDCs) recognition [14][15].

Table 2.15. Cryogel studies.

Application Methods	Application Area	Research Groups	Ref.
Biosensors	Urine samples for microalbumin	Fatoni et al.	[117]
Enzyme purification	Bovineeritrocytes for carbonic anhydrase	Uygun et al.	[118]
Cell culture and tissue engineering	Bone	Inci et al.	[119]
3D cryogel scaffolds	Cultivation of cells	Nilsang et al.	[120]
Depletion studies	Hemoglobin	Derazshamshir et al.	[121]

Cryogels can be used as columns and shape in various sizes, therefore it brings a lot of advantages above on polymers. One of the greatest specialties of the cryogel is removing heavy metal from waters due to their supermacroporous structure. Their high pore volume and large pore size are very useful for separating metal ions from water [17].

Table 2.16. Heavy metal removal studies from waters by cryogel.

Heavy Metals	Heavy Metal Removal Method	Heavy Metal Concentration	Adsorption Capacity	Research Groups	Ref.
Ag(I)	Ag^+ ion imprinted cryogels	1-50 mg/L	49.3 mg/g	Şarkaya et al.	[17]
Cd(II)	Cd(II) ion imprinted cryogels	100 ppm	13.91 mg/g	Jalilzadeh	[122]
Pb(II)	Pb(II) ion imprinted cryogels	100 ppm	17.94 mg/g	Jalilzadeh	[122]
Cu(II)	Cu(II) ion imprinted cryogels	100 ppm	11.20 mg/g	Jalilzadeh	[122]
As(I)	Fe-Al cryogel	0.2 mg/L	24.6 mg/g	Önnby	[123]
Cd(II)	TNT cryogel	0.2 mg/L	157 mg/g	Önnby	[123]
Ni(II)	PHEMA-AC cryogel	20-300 mg/L	22 mg/g	Haktanır	[124]
Cu(II)	PHEMA-AC cryogel	20-300 mg/L	45mg/g	Haktanır	[124]

As we can see from Table 2.16, removing heavy metals by cryogel has many and successful methods. Some of these methods are used as ion imprinted and their removal success is very high because of their adsorption capacities. PHEMA-AC and TNT methods are also very usefull applications for heavy metal removal. These application methods have very high efficiency for adsorption.

3. MATERIALS AND EXPERIMENTS

3.1. Materials

2-Hydroxyethyl methacrylate (HEMA) and poly ethylene glycol diacrylate (PEGDA) was obtained from Sigma (St. Louis, MO, USA), N,N,N,N-tetra-methylethylenediamine (TEMED), ammonium persulfate (APS) were from BioRad (Hercules, CA, USA) and rest of the chemicals were provided from Merck AG (Darmstadt, Germany). The purified water owned a particular conductivity of 18 mS/cm. Before using, glasswares were cautiously disinfected with dilute nitric acid.

The sepiolite minerals used were taken from lacustrine units in the countryside of Türktaciri village of Polatlı district of Ankara province. Sepiolite levels alternate with lacustrine carbonate rocks. Carbonate minerals (calcite, dolomite) are encountered in sepiolite-rich levels up to 30% by volume.

3.2.Purification of Sepiolite

Sepiolite-rich rocks, which are moist due to their structure, were sized first by using a hammer and then left to dry for 48-72 hours under room conditions. Dry sepiolite rock fragments were crushed to smaller sizes by jaw crushers and hand-milled in agate mortars. The milled material was sieved to <63 μm, 63-125 μm, 125-250 μm, 250-500 μm and >500 μm by wet sieving method and each size range was kept in separate packages.

During the experimental studies, materials with the highest surface area (<63 μm) were used. In order to eliminate the carbonate impurities contained in the ground material, it was kept in 10-20% HCl solution which was rotated at 100 rpm at a temperature of 50-75 °C. After the dissolution of the carbonate minerals, the sample powders were washed with purified water in an ultrasonic bath until acid residues were removed.

After washing, the filtered sample powders were plastered onto filter papers to obtain a large surface area and calcined at 220 °C for 48 hours. Sepiolite, which

lost both meteoric and crystalline water, was re-milled for the last time since it re-solidified into thin leaves following drying. The powder samples obtained by grinding were reduced to <63 μm by dry sieving. The obtained pure sepiolite tubular nanocrystals were characterized using SEM-EDS (Carl Zeiss EVO 50 EP - Bruker Xflash 3001 SDD).

3.3. Synthesis of Sepiolite Embedded Composite Cryogels

Sepiolite tubular nanocrystals (60-150 μm; 20, 50, 100 and 200 mg particles in 1 mL solution) of 1 mmol of 2-hydroxyethyl-methacrylate (HEMA) and 5 mmol of PEGDA as crosslinker was added to the monomer solution in the ice bath.

The polymerization was applied for 24 h at -16°C in 50 mL of plastic tubes with a diameter of 3.0 mm using (APS and TEMED, 1% w/v) respectively as initiator and activator. As a control, cryogels without sepiolite tubular nanocrystals were prepared under the same conditions. The cryogel composites, which reached room temperature after polymerization, were washed to remove monomers which did not interfere with the 10% ethanol solution and were dried in a lyophilizer until use and stored at room temperature.

3.4. Characterization of Sepiolite Embedded Composite Cryogels

The size distribution and dispersity of the sepiolite tubular nanocrystals were checked with Zetasizer (Nano S, Malvern Instruments, London, UK), which measures the average format and polydispersity index of the sepiolite particles. The particular surface area was analyzed by multi-point analysis by the BET model. Cryogel pore volume and mean pore diameter were determined by mercury porosimetry (Carlo Erba Model 200, Italy). To determine the equilibrium swelling rate, the dry cryogel was weighed on a balance operating at ± 0.0001 precision and mixed with 50 mL of distilled water. The vessel was kept in a constant temperature water bath for 24 hours (25 ± 0.5°C).

After that, the cryogel was hold up and drops on the surface was took out by means of filter paper, then and it was weighed. Wet and dry weights were booked and cryogel's water ingredient (%) was determined according to $[(W_S-W_0)/W_0]$ equivalence. Here, W_0 and W_S denote the weight of the cryogel after and before

buffing. FTIR (Nicolet iS10, Thermo Fisher Scientific, USA) was operated for chemical structural characterization of cryogel. SEM was employed to characterize the size, accidence of both sepiolite tubular nanocrystals and composite cryogel. Micro-computed tomography device (Bruker Skyscan 1272) was used and the 3-dimensional structure was put forward and further visual analyzes were performed, for the purpose of adjust the amount of macroporosity.

3.5. Heavy Metal Removing from Water

3.5.1. Effect of Time

The composite cryogel (S8) containing sepiolite was illustrated with 100 mL of water for 4 hours. Subsequently, 100 mL of Fe, Ni, As, Cd and Pb solutions at a concentration of 1000 ppb was pumped through to the column under recirculation for 2 hours. The solution's flow value was 1 mL/min. Samples were taken by the standard solution passed through the column at 0, 5, 10, 15, 30, 45, 60, and 120 minutes and examined by ICP-MS (Thermo). The adsorption quantity for all samples was followed by observing the decrease in ICP-MS. Adsorbed each element'squantity was calculated as;

$$Q=[(Ci-Cf)*V]/m \qquad \text{Eq.1}$$

In the calculation, Q is the quantity of adsorbed element onto cryogel's unit mass (µg/g); Ci is concentration of the initial solution and Cf is concentration of the final solution (µg/mL); V is aqua volume (mL), m is the used cryogel's mass (g). These experiments were performed three for statistical calculations and quality control.

3.5.2. Effect of Concentration

The composite cryogel (S8) containing sepiolite was illustrated with 100 mL of water for 4 hours. Subsequently, 100 mL of Mn, Ni, As, Se, Cd, Sb, Co solutions at a concentration of 50-1000 ppb was pumped through to the column under recirculation for 30 minutes. The solution's flow value was 1 mL/min. Samples were taken from the standard solution passed into the column at the end of the incubation time and examined by ICP-MS, Thermo. The adsorption quantity for all samples was followed by observing the decrease in ICP-MS. Adsorbed each element's quantity was calculated as;

$$Q=[(Ci-Cf)*V]/m \quad \text{Eq.2}$$

In the calculation, Q is the quantity of adsorbed element onto cryogel's unit mass (µg/g); Ci and Cf is concentration of the solution (µg/mL); V is the water phase's volume (mL), m is the used cryogel's mass (g). These experiments were performed three for statistical calculations and quality control.

3.6. Adsorption Isotherms

This term describes the link between the adsorbent concentration in the balanced solution and the quantity of adsorbate which adsorbed to the solid phase. Adsorption proceeds until there is a balance between the adsorbent concentration collected on the adsorbent surface and the remaining adsorbate concentration in the solution, this balance is explained by the adsorption isotherms. Adsorption models of Langmuir and Freundlich are performed to determine the interaction of adsorbed molecules with the adsorbent.

Langmuir adsorption isotherm is defined by Equation 3. This model expects that the molecules bind to a certain quantity of regions, each capable of binding only one molecule and these regions are equivalent in energy and also there is no effect these molecules adsorbed in neighboring regions.

$$Q=Q_{max}*b*C_e/(1 + b*C_e) \quad \text{Eq.3}$$

Q is the capacity of elements that bind to the cryogel (mg/ml), Ce is the element conctration in the solution (mg/g), b is constant of Langmuir (ml/mg) and Q_{max} is the highest adsorption capacity (mg/g). When it is linearized, achieved equality is:

$$1/Q_e=1/(Q_{max}*b) * (1/C_e) + 1/Q_{max} \quad \text{Eq.4}$$

The point where the 1/Q graph crosses the y-axis against 1/Ce gives the value of 1/Qmax and the slope gives the value of 1/Qmax * b.

Freundlich equation 5 assumes that the binding of the adsorbent to the adsorbent varies depending on if the adjacent binding regions are full.

$$Q_{eq}=K_f*C_{eq}^{1/n} \quad \text{Eq.5}$$

In this equation, Q_{eq} is the amount of adsorption (mg/g) and Ce is the balance concentration in the solution (mg/l). K_f and 1/n are Freundlich constants which are indicating adsorption capacity and adsorption intensity. When this equation is taken as the logarithm of both sides, equation 6 is obtained.

$$\ln Q_{eq}=\ln K_f + 1/n \ln C_{eq} \quad \text{Eq.6}$$

Experimental data were adapted to Freundlich model and $\ln C_{eq}$ was plotted against $\ln Q_{eq}$. Adsorption constants were calculated from the cut-off point and slope [125][126].

3.7. Adsorption Kinetics

The speed control mechanism can change according to three possible mechanisms during the adsorption process: (1) Film diffusion process or external surface mass transfer in the initial stages of the adsorption process. (2) This stage is followed by reaction or constant speed step. (3) In the last stage, the intra-pore diffusion step is occurred where the adsorption process decreases significantly. These speed control mechanisms are explained by the pseudo-first-order kinetic model (controlled with diffusion) and the pseudo-second-order kinetic model (controlled with chemicals).

The step determining the adsorption rate is compatible with analyte and its diffusion to the adsorbent surface is compatible with the adsorption process pseudo-first order adsorption model. In conditions where the interaction among the analyte and the adsorbent determining the adsorption rate, the adsorption process is compatible with the pseudo-second order kinetic model. The adsorption process is called diffusion controlled in the first kinetic model; it is called chemically controlled in the second kinetic model.

Interaction time is important to figure out the steps that affect the velocity of the adsorption process. Mechanisms that control this process are mass transfer and chemical reaction. In determining these mechanisms, pseudo 1st and 2nd order kinetic models were applied to the experimental data. It is expected that the restrained concentrations are equal to the surface concentration of the adsorbent. 1st order speed equation is the most commonly calculated equation in the adsorption of solute from liquid solution. The following equation has been applied;

$$dq_t/dt=k_1(q_{eq}-q_t) \quad \text{Eq.7}$$

In Eq.7, k_1 is the pseudo-first order adsorption rate constant (min^{-1}), q_{eq} and q_t are the number of elements adsorbed at balance time and at any time of t (mg/g). When $q_t=0$, at t=0 and $q_t=q_t$, at t=t boundary conditions and integral are applied;

$$\log[q_{eq}/(q_{eq}-q_t)=(k1*t)/2.303 \quad \text{Eq.8}$$

the above equation is achieved. When equation 8 is linearized by reorganizing:

$$\log(q_{eq}-q_t)=\log(q_{eq})-(k1*t)/2.303 \quad \text{Eq.9}$$

Linearity of the $\log(q_{eq})$ graph to ‘’t’’ shows the practicality of the kinetic model.

Pseudo-second order equation can be explained by adsorption balance capacity is given as below:

$$dq_t/d_t=k_2(q_{eq}-q_t)^2 \quad \text{Eq.10}$$

In equation 10, k_2 is the pseudo-second order velocity constant ($g.mg^{-1}.min^{-1}$). The following equation is obtained by performing the boundary requirements of $q_t=0$ at time t=0 and $q_t=q_t$ at time t=t.

$$1/(q_{eq}-q_t)]=(1/q_{eq})+k_2t \quad \text{Eq.11}$$

The linear state of this equation is;

$$(t/q_t)=(1/k_2q_{eq}^2)+(1/q_{eq})*t \quad \text{Eq.12}$$

In order for the second order kinetics to be practicable, the graph of t/q_t to t must be linear. Speed constant (k_2), equilibrium adsorption (q_{eq}) are obtained from the cut-off point and slope, respectively [127][128].

3.8. Heavy Metal Adsorption from a Certified Water Sample

Separation from multiple pollutant environments is required especially in places where it will be used for purification. For achieving this goal, these procedures were performed in order to control the amount of sepiolite added composite cryogels heavier than the standard solution containing certified multi-elements. The certified multi-element standard solution contains 21 different elements.

4. RESULTS AND DISCUSSION

Sepiolite embedded composite cryogel production is carried out in an almost frozen system, where ice crystals act as porogen and freezing continues apparently in the non-frozen micro-phase of the frozen path.

After gelation is done, which is in the micro phase, the reaction system outcomes of melting in a system of large pores (gapformerly filled by ice crystals) encircled by intense hydrogel barriers consist in unfrozen microphase.

4.1. Characterization of Sepiolite

Since sepiolite re-solidified into thin leaves after drying and also it already lost its crystalline and meteoric water, it was re-milled for the last time.

Provided powder samples were reduced to <63 μm by dry sieving. The obtained pure sepiolite tubular nanocrystals were characterized using SEM-EDS (Carl Zeiss EVO 50 EP-Bruker Xflash 3001 SDD).

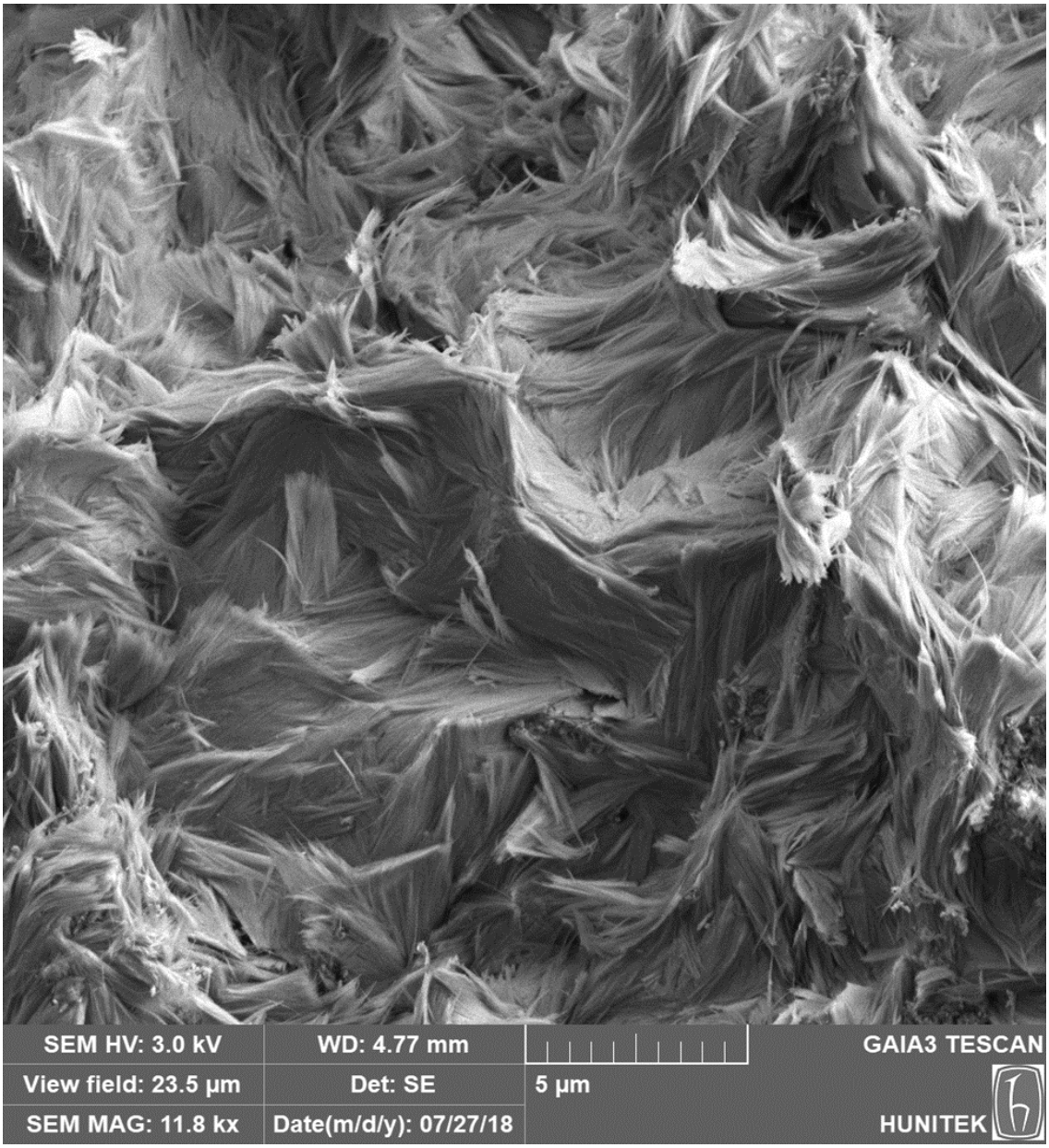

Figure 4.1. Sepiolite before the acid treatment illustrated by 5 µM in scale (SEM).

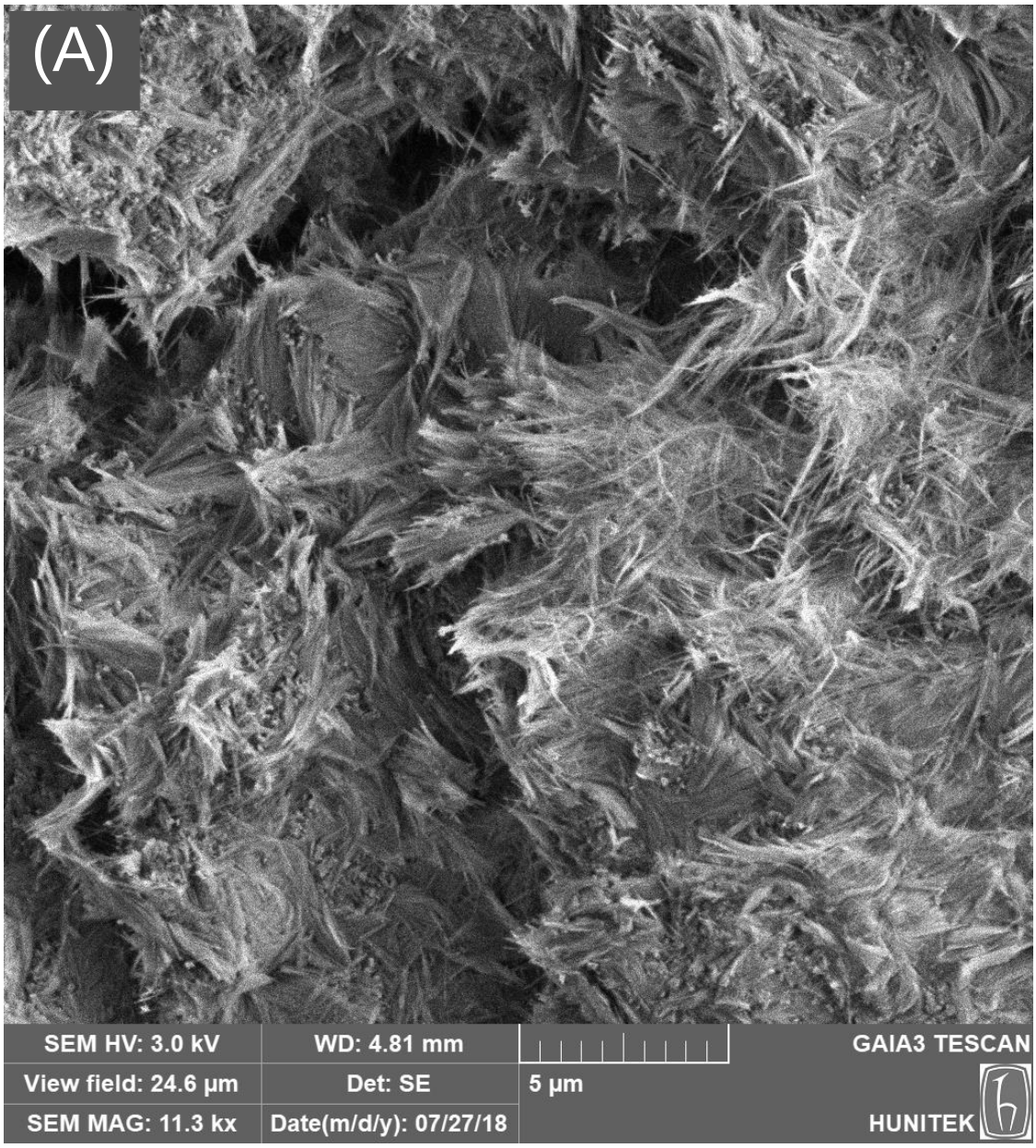

Figure 4.2. Sepiolite after the acid treatment illustrated by 5 µM in scale (SEM).

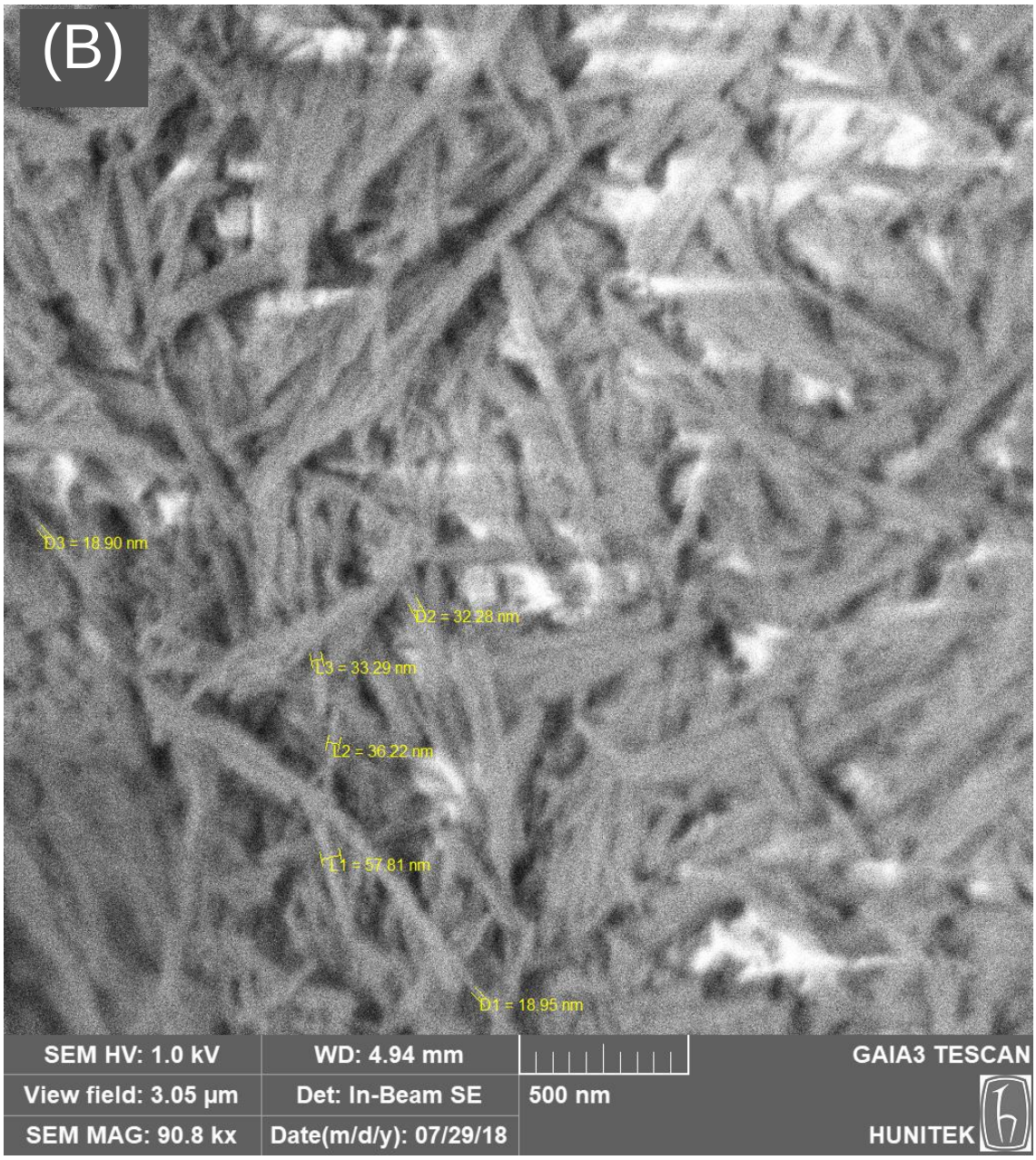

Figure 4.3. Sepiolite after the acid treatment illustrated by 500 nm in scale (SEM).

4.2. Preparation of Sepiolite Embedded Cryogels

Sepiolite tubular nanocrystals (60-150 μm; 200 mg particles in 1 mL solution) of 1 mmol of HEMA and 5 mmol of PEGDA as crosslinker was mixed to the monomer in ice bath. The polymerization was applied for 24 h at -16°C in 50 mL of plastic tubes with a diameter of 3.0 mm using (APS and TEMED, 1% w/v) respectively as initiator and activator. The cryogel composites, which reached room temperature after polymerization, were washed to remove monomers which did not interfere with the 10% ethanol solution and were dried in a lyophilizer until use and stored at room temperature. The schematic procedure of the preparation of cryogels is in Figure 4.4. In addition, the real image of the prepared column is in Figure 4.5.

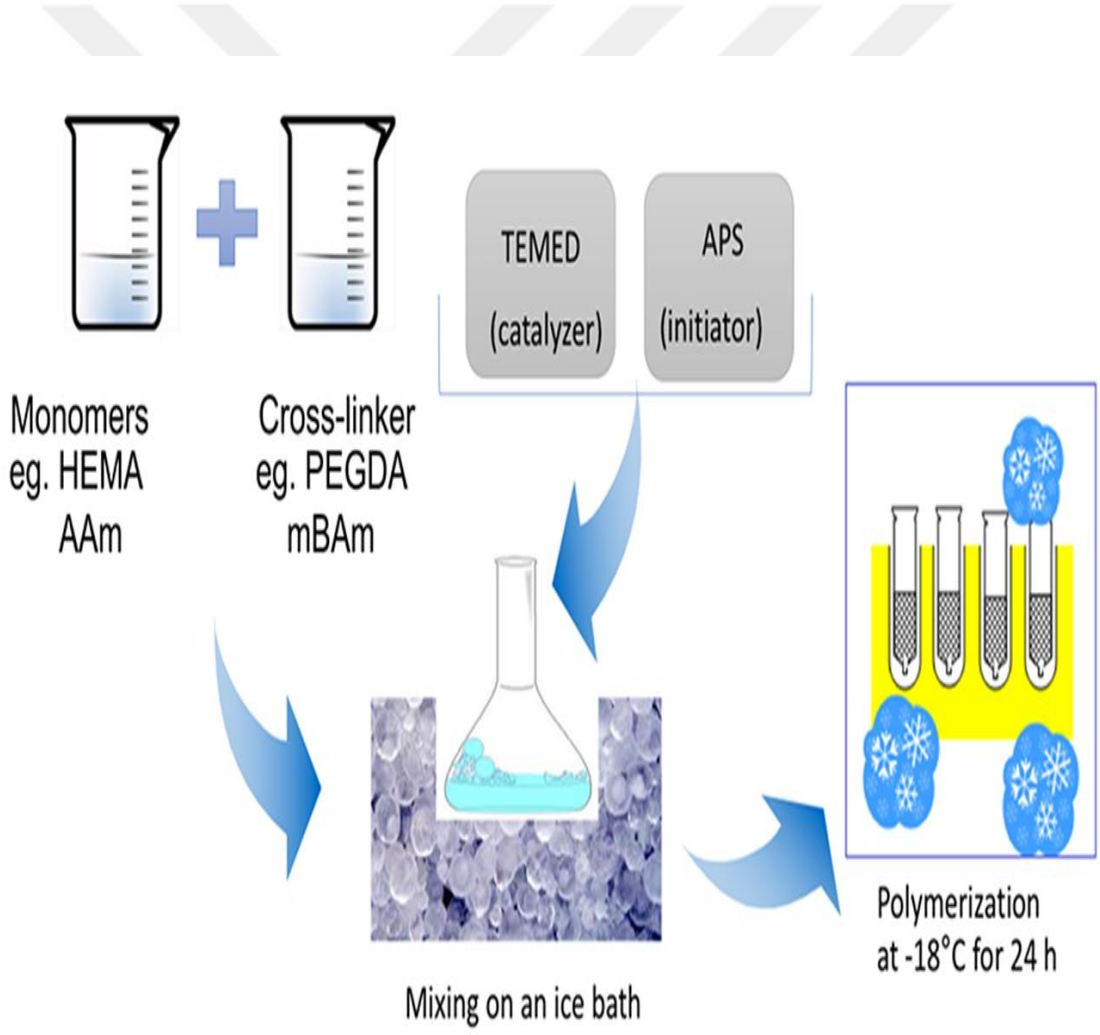

Figure 4.4. Scheme of a typical procedure for cryogel preparation.

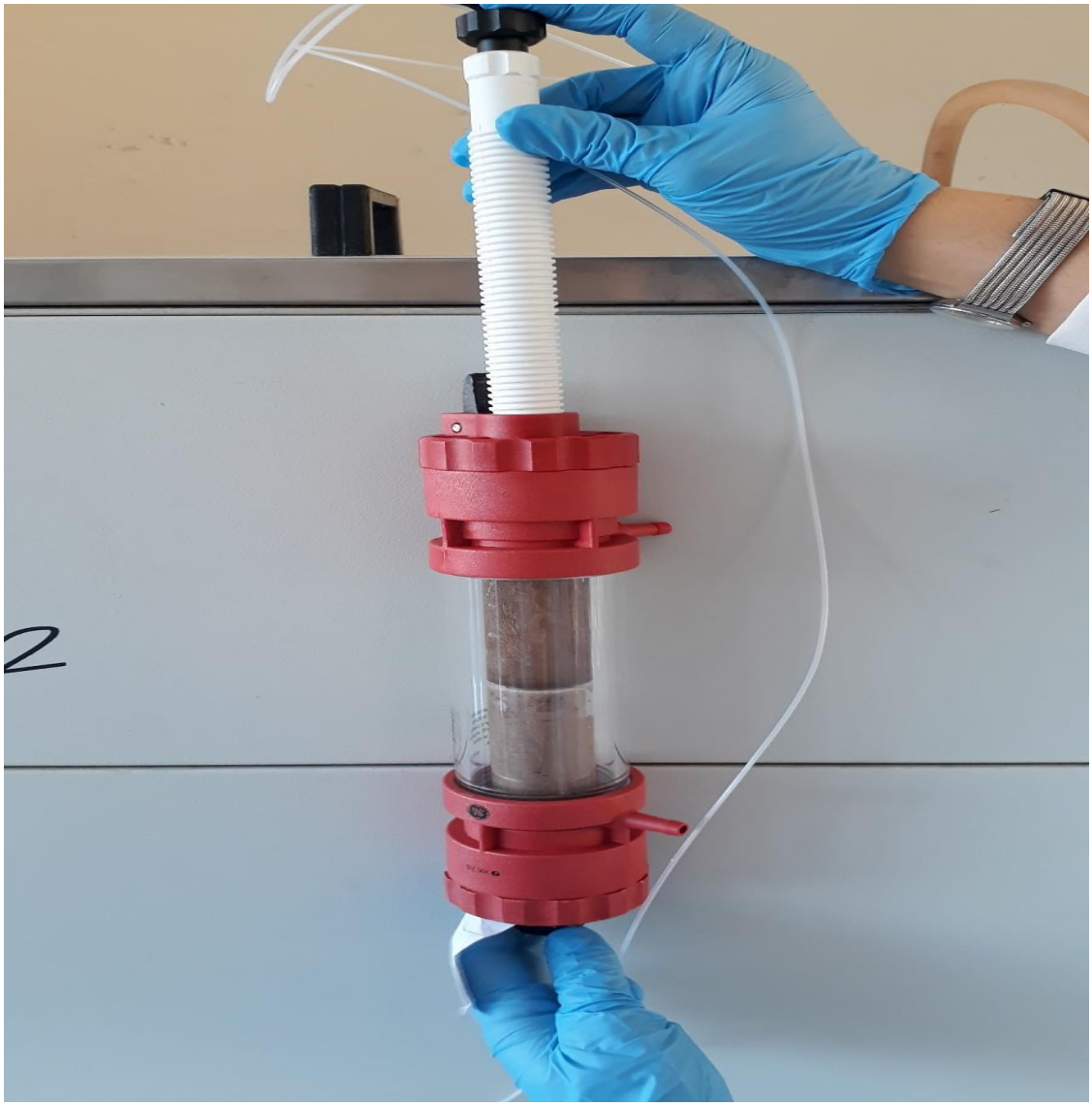

Figure4.5. Photograph of the sepiolite embedded nanocomposite cryogel column.

4.3. Characterization of Nanocomposite Cryogels

Sepiolite-embedded composite cryogels were prepared with cryo-polymerization under zero temperatures. After polymerization, cryogel composites, which reached room temperature, were washed with a 10% ethanol solution to remove unreacted monomers and made ready for use by cutting with 0.8- and 1.2-mm diameter perforators. For characterization studies, it was also left to dry in a lyophilizer and stored at temperature of room. Figure 4.6 shows optical photographs of sepiolite containing cryogel composites prepared in different ratios.

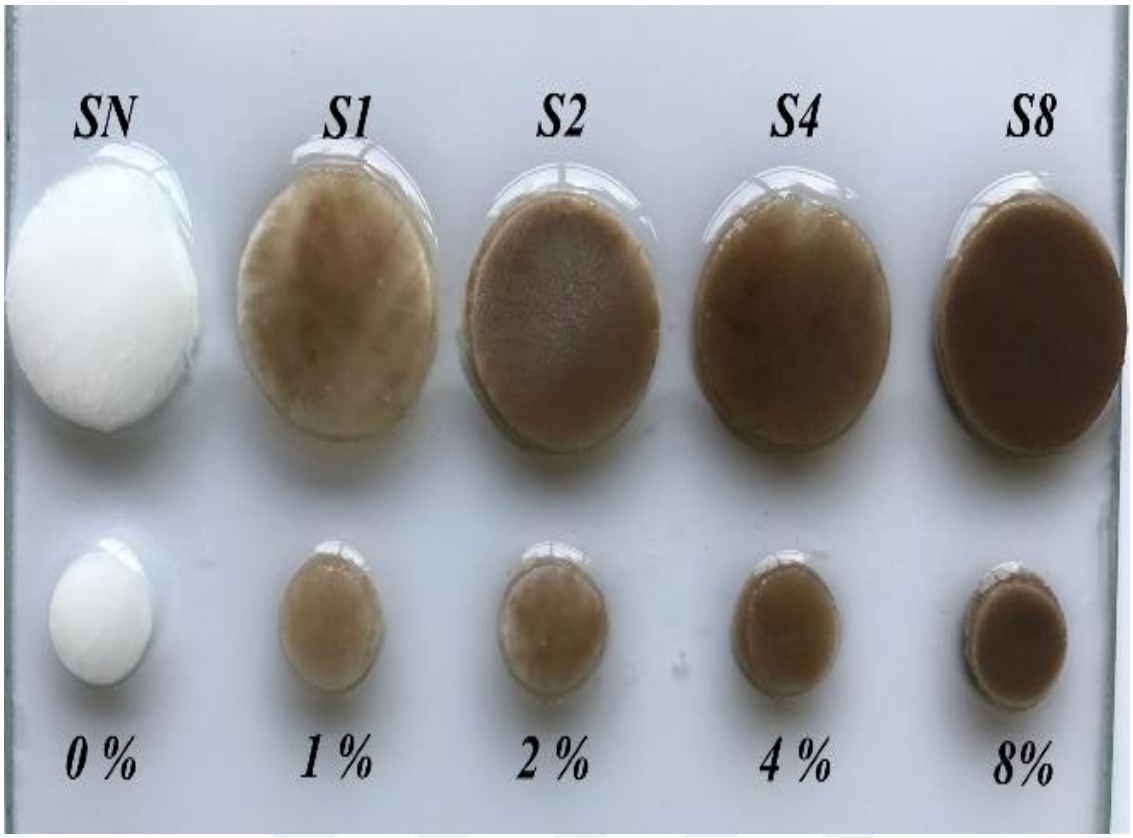

Figure 4.6. Composite cryogel containing sepiolite in different ratios (SN: 0%, S1: 1%, S2: 2%, S4: 4% and S8: 8%).

After the synthesing of cryogels, polymerization actualize in the concentrated melt monomers and unfrozen liquids containing initiator. Ice crystals, which are occured at freezing, like pore. Therefore, the size and the shape of the crystals adjust the physical properties of the pores created. The magnitude of the crystals based on the freezing rate of the system, provided that concentration, volume, geometrical format of the sample must not change [129].

The initial temperature is an important factor in determining freezing rate, at this thesis study all solutions were kept close to 0°C as they were waited in an ice bath with the freezing temparature before mixing. Various measures were taken to obtain a repeatable freezing mold, such as the small size samples and uniform figure (The syringes, which are 50 mL, filled with the final solution, which is 46 mL) were applied. The moments when monomer and initiator were blended (when the polymerization fire up) and the syringes were filled with polymersol which were immersed in the cryostat cooler were fully controlled.

Sepiolite size distribution was examined by using Zetasizer analyzer. According to results, the size distribution of the sepiolite particles was determined to be in the range of 600-1000 nm.

The dense and wide-pore PHEMA cryogel is advantageous when working with viscous liquids and allows smooth fluids flow through the cryogel. This reduces the diffusion resistance and facilitates mass transfer. These properties of PHEMA cryogel enable the analyte-ligand interaction to be affected efficiently in the column. However, large pore diameters are a reason for their low surface area properties and no effective increase in binding capacity is observed [130].

Therefore, the sepiolite-containing PHEMA cryogels prepared within the scope of this thesis were prepared by forming composites in the presence of sepiolite to enhanced the surface area, thus provide high binding efficiency. Table 4.1 shows measurements of BET and pore diameters.

Table 4.1. Surface area measurements.

	BET Surface Area (m^2/g)	D-H Total Pore Surface Area[1] (m^2/g)	BJH Total Pore Volume[2] (cm^3/g)	Average Pore Diameter (Å)
Sepiolite	173.81	55.87	0.032	21.72
SN	25.6	-	-	-
S4	670.12	87.71	0.026	22.02-70.07
S8	1170.78	80.40	0.058	20.91-76.06

[1]D-H Pore Total Surface Area: It was studied between 17 and 3000 Å diameter.

[2]BJH Pore Total Volume: Worked between 17 and 3000 Å diameter.

The S8 cryogel's particular surface area was determined at the value of 1170.8 m^2/g on average in the multi-point analysis according to the BET model, approximately 47 times the surface area of a plain cryogel based on PHEMA (average 25.6 m^2/g) [130]. This result shows that the added sepiolite increases the surface area and the desired target is achieved. The total surface area of the S8 composite cryogel pore is 80.40 m^2/g and the mean pore diameter is between

the values of 20-76 Å, which indicates that the S8 composite cryogel has a macroporous structure. This macroporosity allows the passage of liquids, such as wastewater, even at high flow rates. The mean pore volume and diameter are also supported by SEM images (Figure 4.8).

To determine the equilibrium swelling rate, the dry cryogel was weighed on a balance operating at ± 0.0001 precision and located in a beaker consist of distilled water, which is 50 mL. The PHEMA cryogel's swelling degree balance was changed between 3.03-7.28 g H_2O/g cryogel by changing the crosslinker ratio. PHEMA monolithic cryogel is sponge-like and has elasticity. Similarly, cryogel containing sepiolite has a sponge-like elastic structure. When cryogel is taken up by the hands and tightened up with reasonable pressure, the water accumulated in the pores can be easily removed. Dehydrated and compressed cryogel restored to its original shape and size within the seconds of re-contact with water.

Table 4.2. Equilibrium swelling properties of composite cryogels.

Cryogel	Equilibrium swelling Ratio (%)	Micro-Porosity (%)	Swelling Ratio	Cryogel Formation Yield
SN	83.80	55.63	5.17	88.11
S1	87.93	48.06	7.28	63.62
S2	86.44	45.29	6.37	66.81
S4	79.55	36.04	3.89	64.08
S8	75.20	53.30	3.03	79.45

Cryogels were dehyrated at 60 °C and kept dry almost indefinitely. Water vapor was absorbed by one of the cryogels which are the 88% of cryogel's weight. Cryogels, which are immersed in liquid, were rehydrated in a short time without spoiling their supermacroporous forms. Because of this special ability, cryogels draw all the attention by the mean of chromatographic carriers. The pore volume

is one of the important abilities of chromatographic substance. 3–4% of the fully dried cryogel's total weight is dry polymer.

The adsorbed water from vapor, which is closely bound by polymer, constitutes approximately 4–5% of the weight. Water, which is closely connected by polymer, creates the walls of pore. Therefore, the water in the pore's accounts for 80% of the remaining cryogel weight. Because of the flexible cryogels, a serious quantity of water in the pores can be mechanically tightened from swollen monolithic models. Because of this, the basic region of the cryogel volume consist of the interconnected supermacropores.

Structural analysis of sepiolite, sepiolite-free (SN) and sepiolite-containing (S8) composite cryogels was examined in the FTIR spectrum in between the value of 4000-600 cm^{-1} (Figure 4.7). The characteristic peaks of SN cryogel are at 3424 cm^{-1} (O-H stretch), 2951 and 2873 cm^{-1} (C-C stretch), 1720 cm^{-1} (C=O stretch) and 1242 and 848 cm^{-1} (C-O and C-O-C) frequencies. The characteristic peaks of the S8 composite cryogel are 3385 cm^{-1} (O-H stretch), 2950 and 2875 cm^{-1} (C-C strain), 1721 cm^{-1} (C = O strain) and 1156 and 881 cm^{-1} (C-O and C-O-C stretching) frequencies. And also, the characteristic peak at 1436 cm^{-1} seen in the sepiolite confirmed the incorporation of the sepiolite into the S8 composite cryogel.

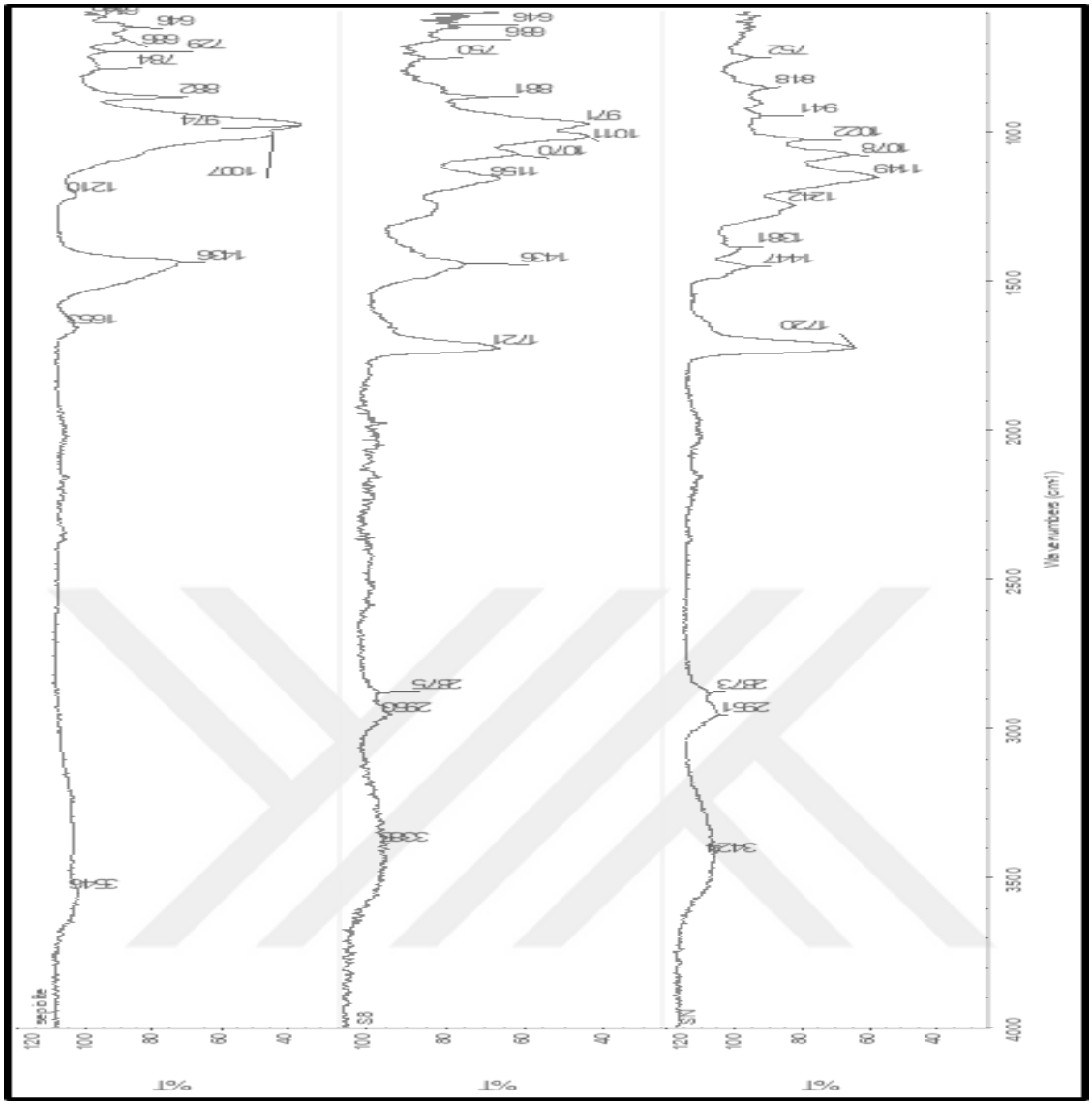

Figure 4.7. The FTIR spectra of sepiolite (Sep), sepiolite-free (SN) and sepiolite-containing (S8) composite cryogels between the values of 4000-600 cm^{-1}.

The ice crystals shaped during the formation of a PHEMA-based plain cryogel melt the cryogel to room temperature when the polymerization process comes to an end to form the interconnected porous polymer network.

The diameters of these interconnected pores vary in the range of approximately 10-200 μm depending on the polymerization conditions. The SEM image of the composite cryogels without sepiolite (A, SN) and containing 8% sepiolite (B, S8) is indicated in Figure 4.8.

Although the interconnected pore structure between the values of 10-100 μM is shown in Figure 4.9A layered structural image is formed after sepiolite enters the cryogel structure (Figure 4.9B). The multilayered structural image of S8 composite cryogel containing sepiolite is supported by mCT analysis (Figure 4.9).

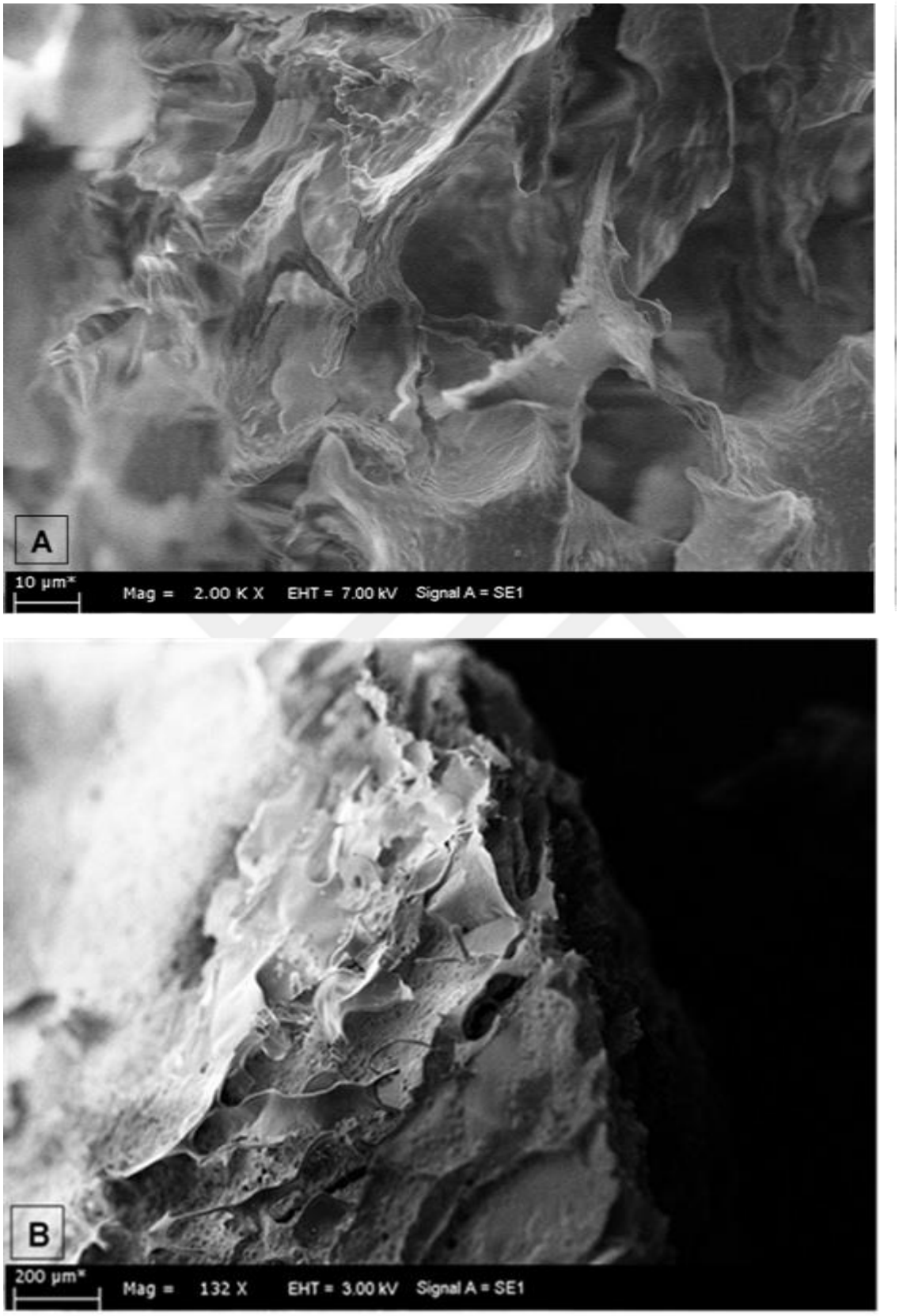

Figure 4.8. (A) SN Cryogel and (B) S8 Cryogel images of SEM.

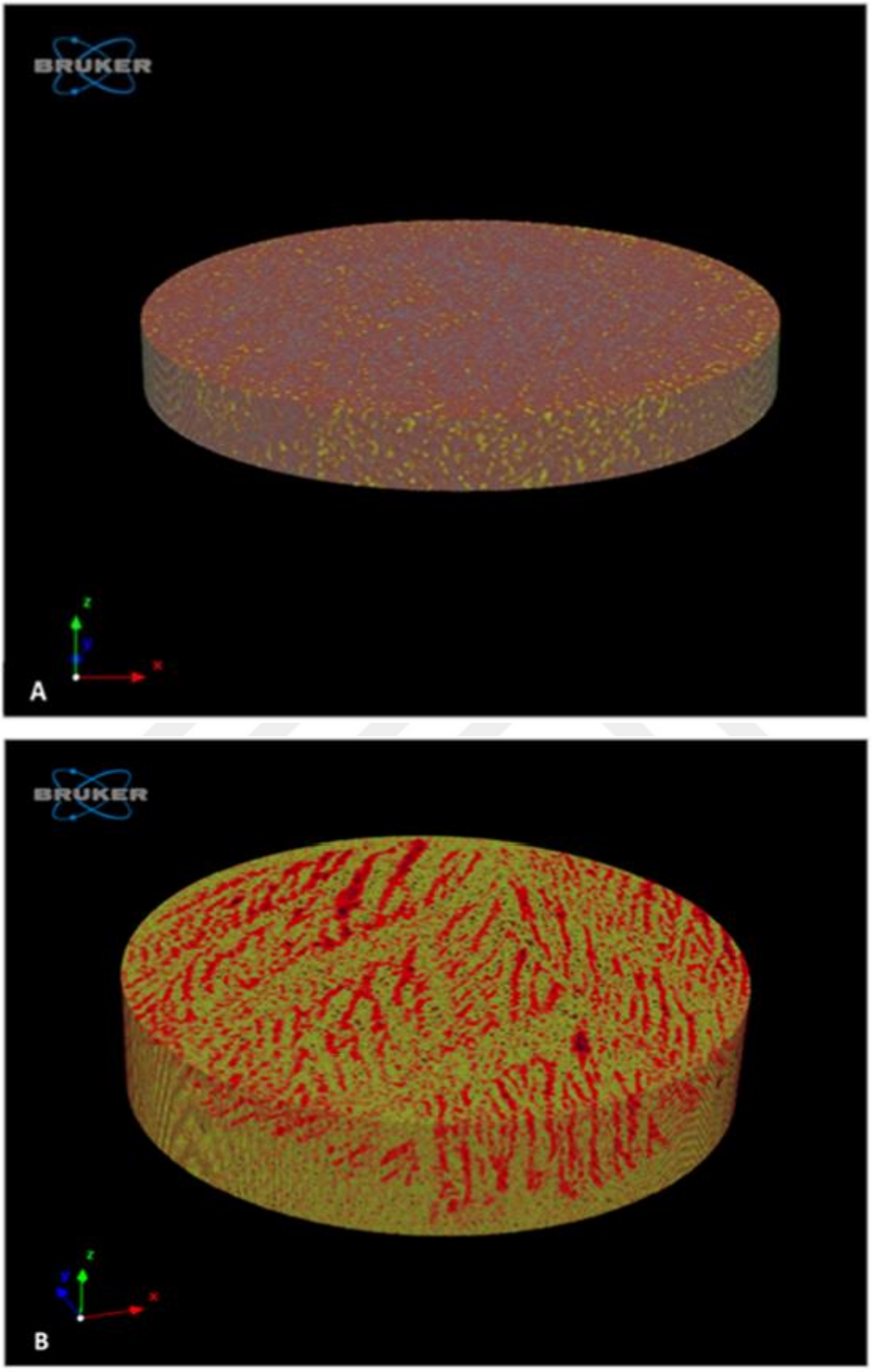

Figure 4.9. Micro-computed tomography (μCT) Analysis (A) SN Cryogel (B) S8 Cryogel.

4.4. Heavy Metals Adsorption Studies

4.4.1. Effect of Time

100 mL of heavy metal solutions containing Mn, Ni, As, Se, Cd, Sb and Co at a concentration of 1000 ppb were pumped from the compound cryogel columns under recirculation for 2 hours. Under a constant flow rate, samples were taken from the standard solutions passed through the columns after 0, 5, 10, 15, 30, 45, 60 and 120 minutes and analyzed by ICP-MS. The amount of 7 different heavy metal adsorption of cryogel columns against time is stated in Figure 4.10.

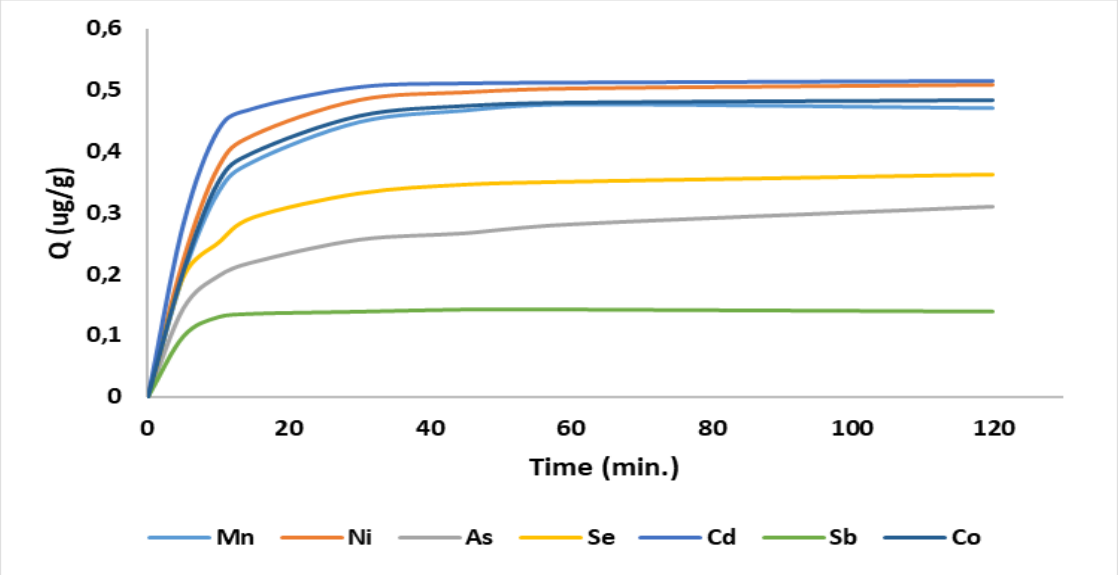

Figure 4.10. Changing of Heavy Metal Adsorption Capacity Over time for sepiolite embedded cryogel (50 ppb, 25°C, 1 mL/min).

4.4.2. Effect of Concentration

As shown in Figure 4.10, the composite cryogel absorbed 97% of all metals in water after 30 minutes. The adsorption capacity of heavy metals on composite cryogels increased with increasing consantrations of heavy metals and composite cryogel tend to reach adsorption plateau as aspected. It was observed that, the maximum adsorption capacities of composite cryogels for all heavy metals were the highest value due to the higher sepiolite amount (S8). As shown in Figure 4.11, the capacity of max binding was monitored at 30 minutes. So, it can be said that 30 minutes will be sufficient for maximum binding capacity.

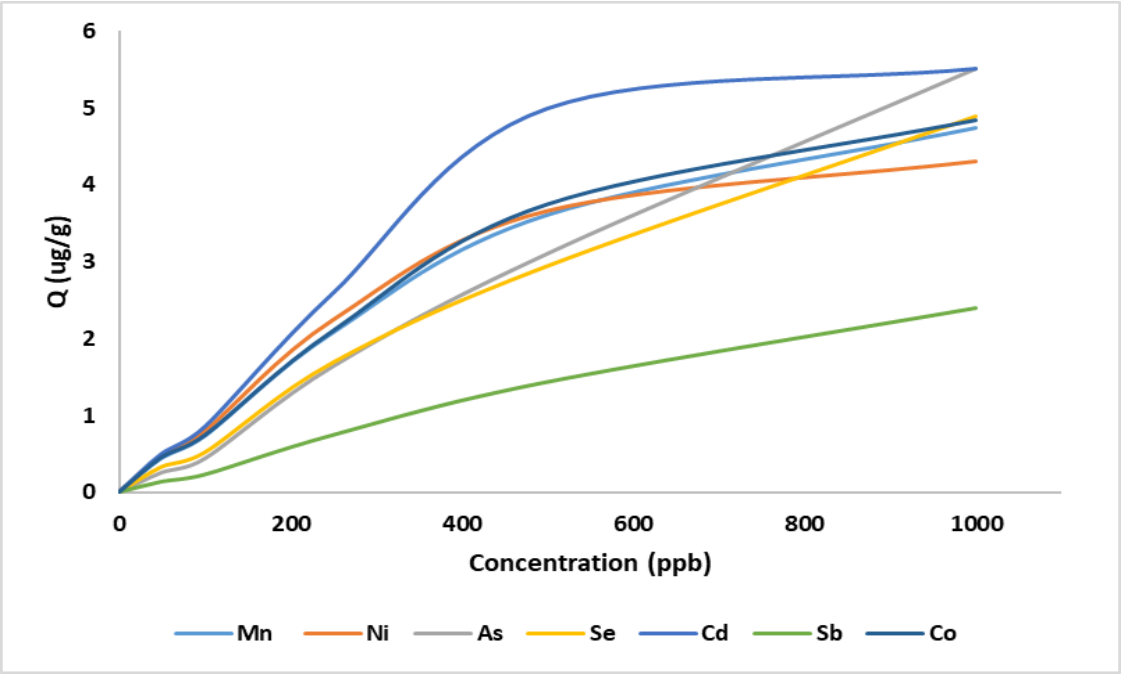

Figure 4.11. Changing of Heavy Metal Adsorption Capacity Over Concentration for sepiolite embedded cryogel (2 Hours, 25°C, 1 mL/min).

4.5. Adsorption Isotherms

Langmuir adsorption isotherm is defined by Equation 13. This model expects that the molecules bind to a certain quantity of regions, each capable of binding only one molecule and these regions are also equivalent in energy. This model also assumes it has no effection between molecules adsorbed in neighboring regions.

$$Q=Qmax * b * Ce/(1 + bCe) \quad \text{Eq.13}$$

In Eq.13, Q is the number of elements that bind to the cryogel (mg/g), b is the Langmuir constant (mL/mg), Ce is the equilibrium concentration (mg/mL) and Qmax is the highest adsorption capacity (mg/g). When it is linearized, the equation below is obtained:

$$1/Q_e=1/(Q_{max}*b)(1/C_e) + 1/Q_{max} \quad \text{Eq.14}$$

The point where the 1/Q graph crosses the y-axis against 1/Ce gives the value of 1/Qmax and the slope gives the value of 1/Qmax.b (Figure 4.12 and 4.13).

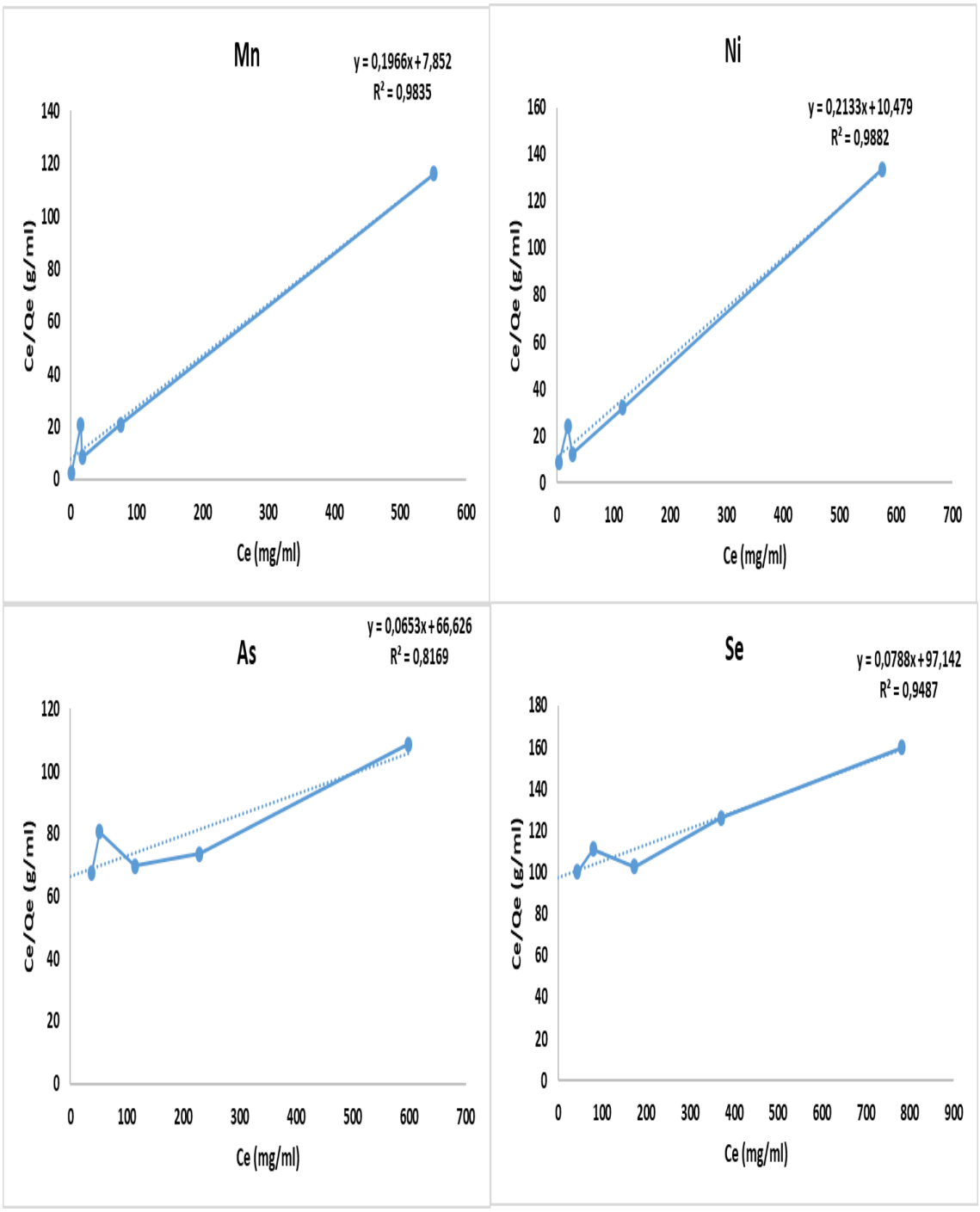

Figure 4.12. Langmuir isotherm curves of the elements.

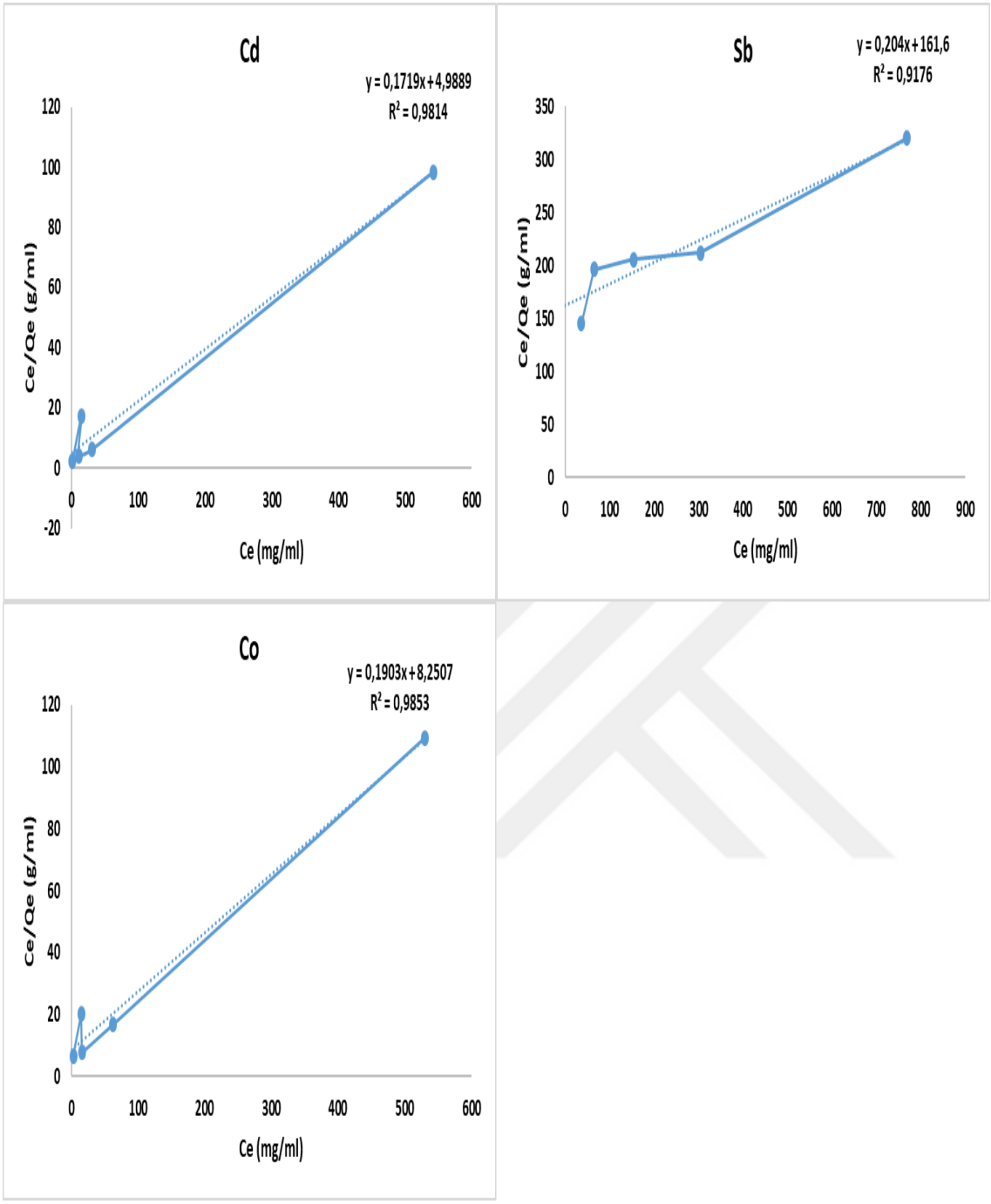

Figure 4.13. Langmuir isotherm curves of the elements.

Freundlich equation (Figure 4.12 and Figure 4.13) assumes that the binding between the adsorbent varies depending on whether the adjacent binding regions are full.

Qeq=Kf*Ceq*1/n Eq.15

In this equation, Qeq is amount of adsorption (mg/g) and Ce is the balance element concentration (mg/L). Kf and 1/n are Freundlich constants show ads capacity and intensity.

$$\ln Qeq = \ln Kf + 1/n \ln Ceq \qquad \text{Eq.16}$$

Experimental data are adapted to Freundlich model and lnCeq is plotted against lnQeq (Figure 4.14 and Figure 4.15). Adsorption constants were calculated from the cut-off point and slope.

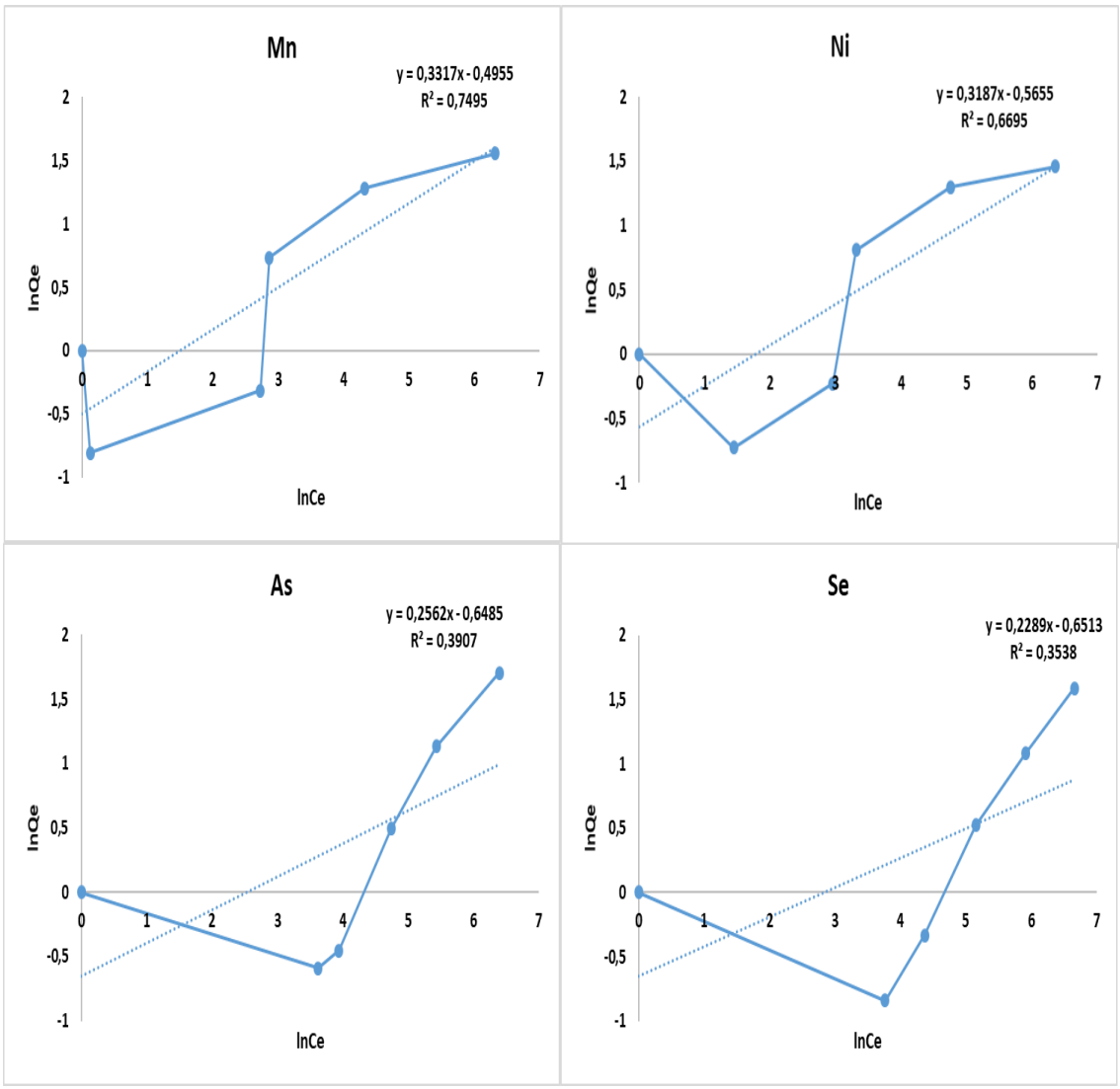

Figure 4.14. Freundlich isotherm curves of the elements.

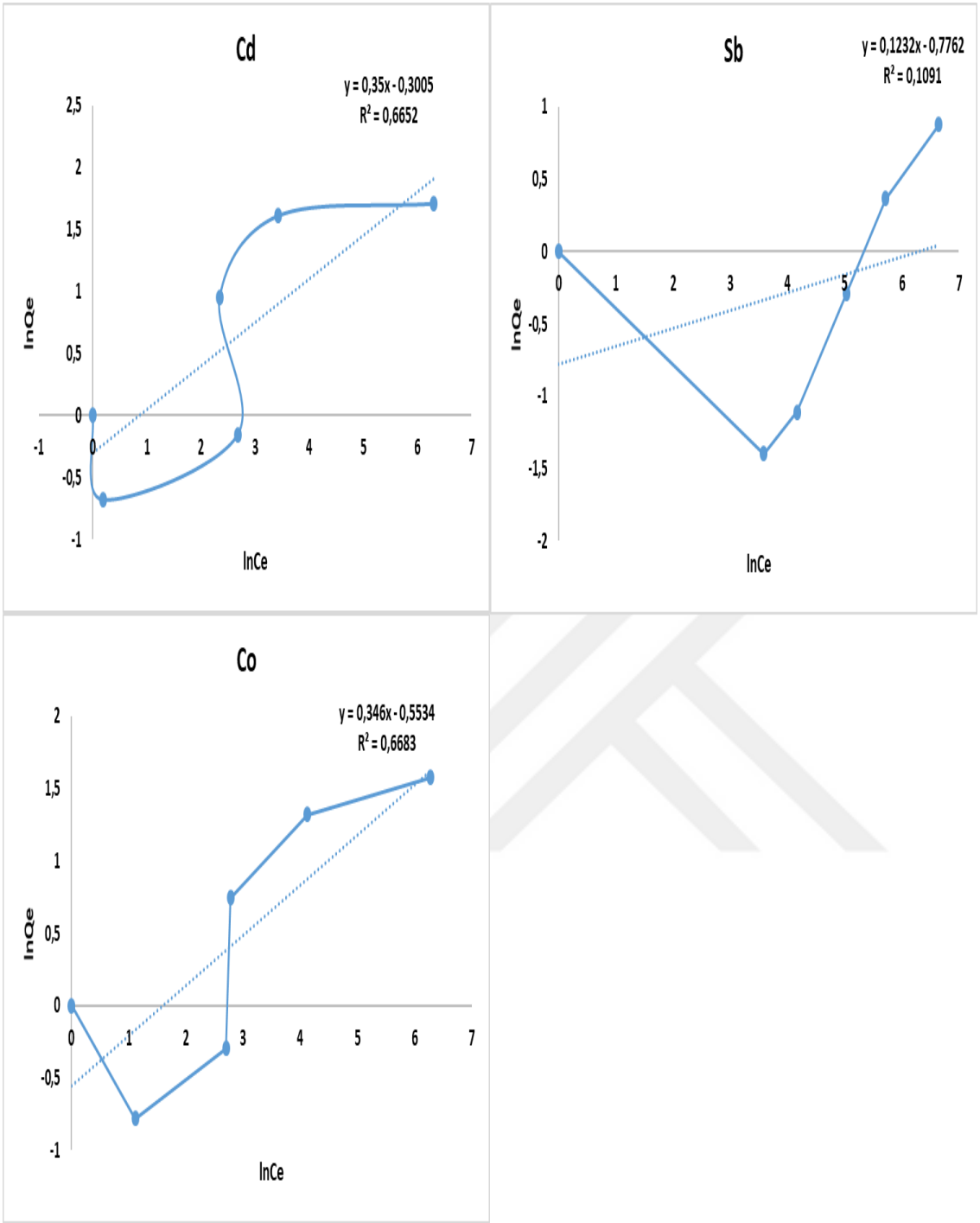

Figure 4.15. Freundlich isotherm curves of the elements.

Table 4.3. The experimental binding capacity (Qexp) found and Langmuir and Freundlich constants calculated for Mn, Ni, As, Se, Cd, Sb, and Co.

	Experimental	Langmuir Constants			Freundlich Constants		
	Q_{exp} (µg/g)	Q_L (µg/g)	b (mL/µg)	R^2	K_F (µg/g)	n	R^2
Mn	4.74	5.08	0.025	0.9835	1.64	3.01	0.7495
Ni	4.30	4.68	0.02	0.9882	1.76	3.13	0.6695
As	5.50	15.31	0.0009	0.8169	1.91	3.90	0.3907
Se	4.88	12.69	0.0008	0.9487	1.92	4.36	0.3538
Cd	5.52	5.81	0.034	0.9814	1.35	2.85	0.6652
Sb	2.40	4.90	0.0012	0.9176	2.17	8.11	0.1091
Co	4.84	5.25	0.023	0.9853	1.73	2.89	0.6683

Calculated numbers for isotherms are given in Table 4.3. Show the writen datas, the adsorption process from the correlation coefficients fit the Langmuir adsorption model for Mn, Ni, As, Se, Cd, Sb and Co. In addition, the maximum adsorption value calculated from isotherm results matches the experimental data.

4.6. Adsorption Kinetics

Interaction time is important to figure out the steps that affect the velocity of the adsorption process. Mechanisms that control the process are mass transfer and chemical reaction. In determining these mechanisms, pseudo 1st and 2nd order kinetic models were applied. It is showed the calculated concentration are equal to the adsorbed concentration of the adsorbent. Lagergren's 1st degree velocity

equation is the most commonly applied equation in the ads of solute in aqua media. It is shown with the following equation;

$$dq_t/dt=k_1(q_{eq}-q_t) \quad \text{Eq.17}$$

In equation 17, k_1 is the pseudo-first order adsorption rate constant (min^{1-}), q_{eq} and q_t are the amount of elements adsorbed at equilibrium time and at any time of t (mg/g);

$$\log[q_{eq}/(q_{eq}-q_t)]=(k_1 * t)/2.303 \quad \text{Eq.18}$$

Equality 18 can be linearized by rearranging;

$$\log(q_{eq}-q_t)=\log(q_{eq}) - (k_1 * t)/2.303 \quad \text{Eq.19}$$

Linearity of the $\log(q_{eq})$ graph to t shows the applicability of the kinetic model (Figure 4.16 and 4.17). In the pseudo-first-order kinetic expression, $\log(q_{eq})$ must be equal to the cut point of the ordinate axis of the $\log(q_{eq}-q_t)$ graph to t.

Pseudo-second order equation originates from adsorption balance capacity can be given as below:

$$dq_t/d_t=k_2(q_{eq}-q_t)^2 \quad \text{Eq.20}$$

In equation 20, k_2 is the pseudo-second order velocity constant ($g.mg^{1-}.min^{1-}$). The following equation is obtained by using the boundary conditions of $q_t=0$ at time t=0 and $q_t=q_t$ at timet=t in equality.

$$1/(q_{eq}-q_t)]=(1/q_{eq}) + k_2 * t \quad \text{Eq.21}$$

The linear state of this equation is below;

$$(t/q_t)=(1/k_2 q_{eq}^2) + (1/q_{eq}) * t \qquad \text{Eq.22}$$

For second order kinetics to be applicable, the graph of t/q_t must be linear against t (Figure 4.18). Speed constant and equilibrium adsorption is taken from cut-off point and slope.

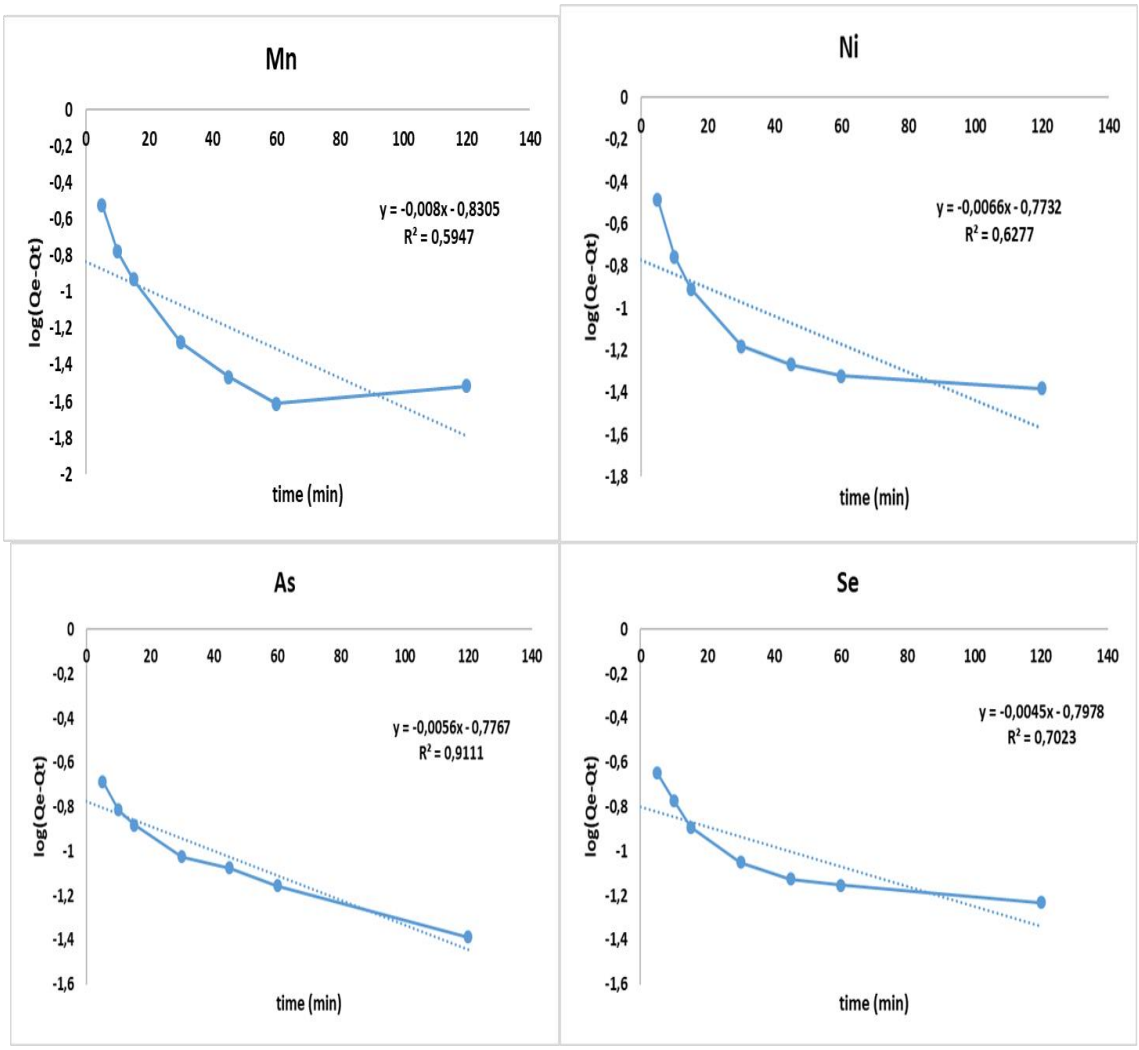

Figure 4.16. Graphs of pseudo-first order adsorption kinetics for the adsorption of elements.

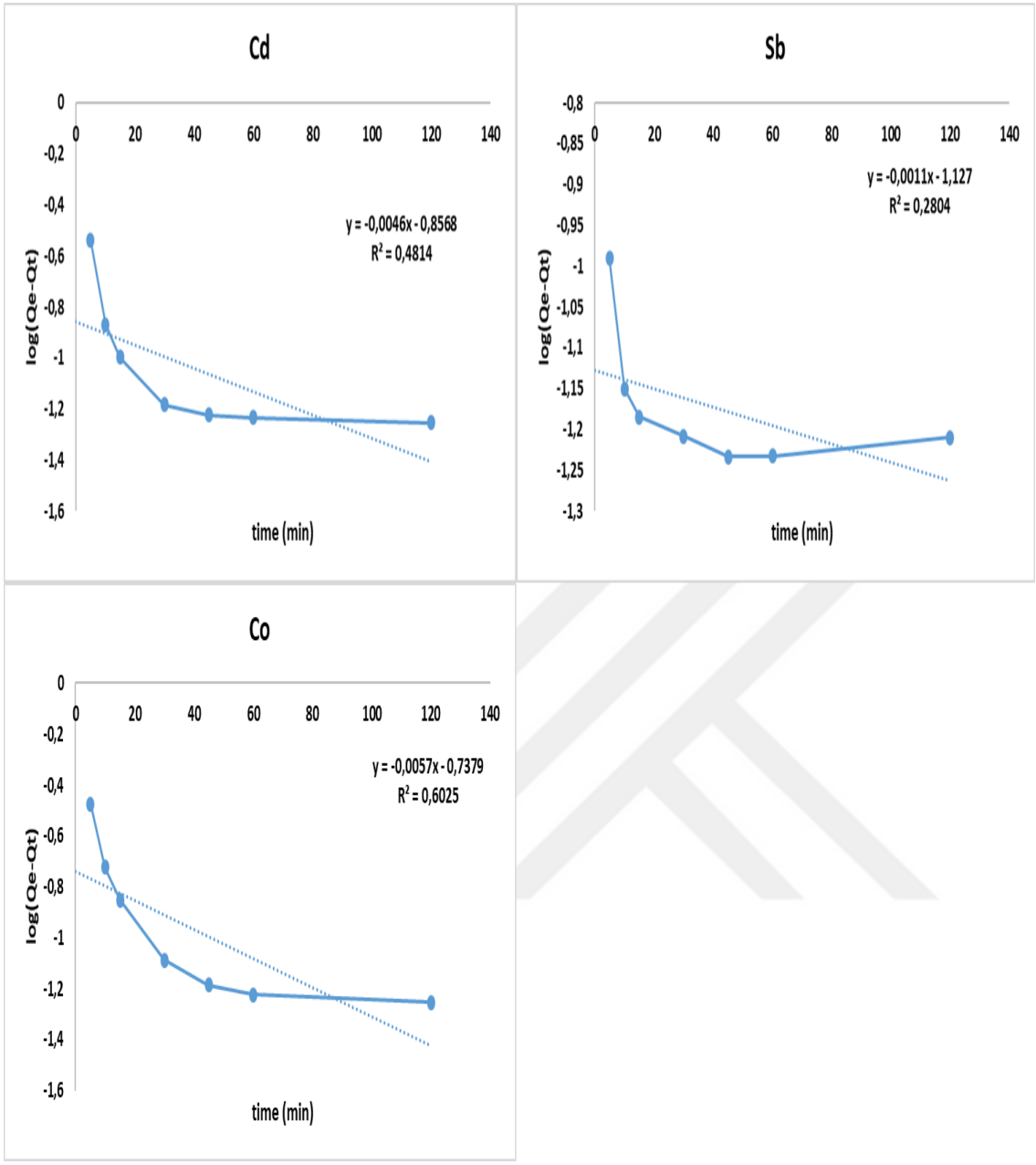

Figure 4.17. Graphs of pseudo-first order adsorption kinetics for the adsorption of elements.

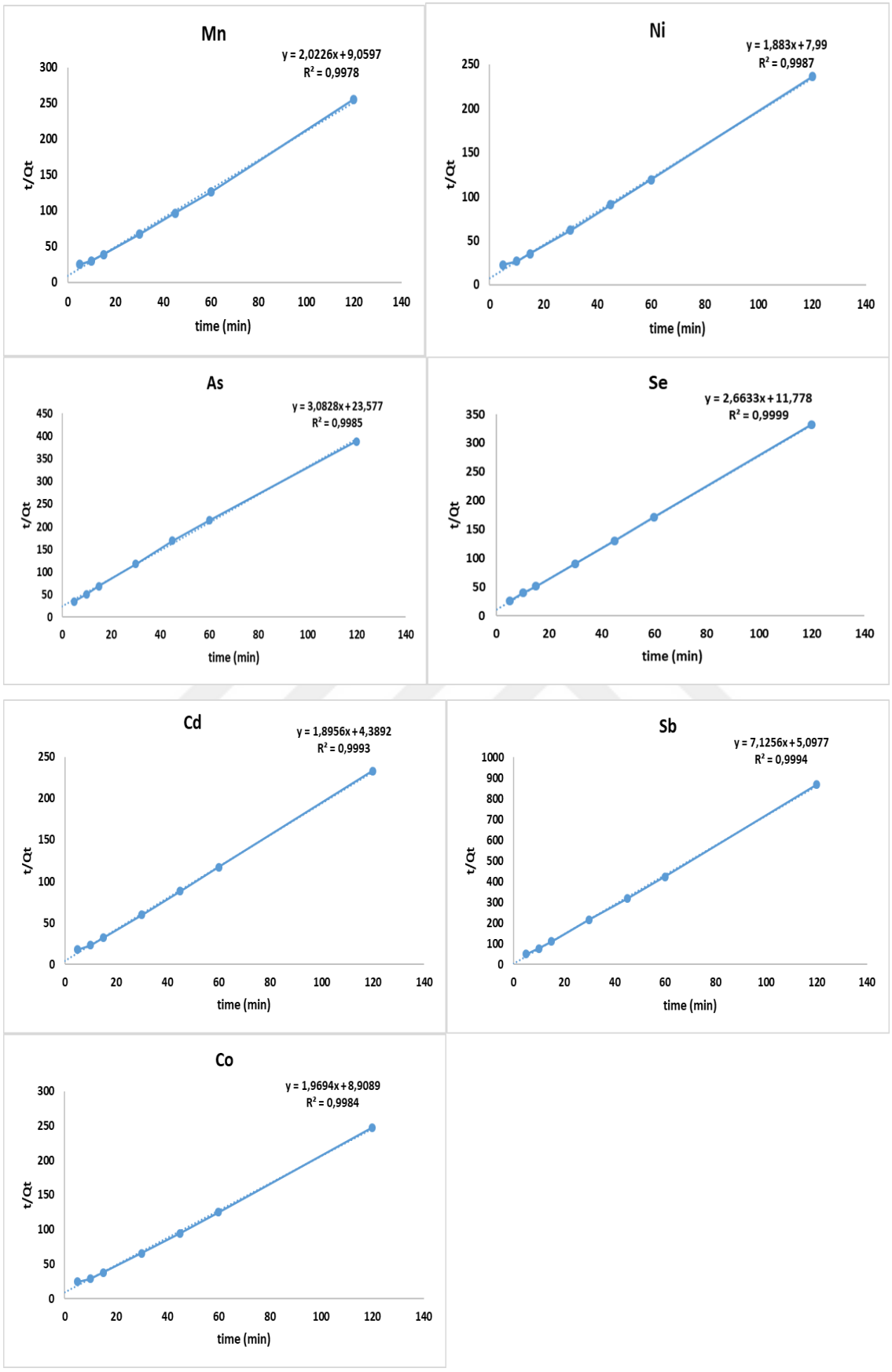

Figure 4.18. Graphs of pseudo-second order adsorption kinetics for the adsorption of elements.

The pseudo-first and pseudo-second-order kinetic parameters calculated from the kinetic analysis data of the 7 different elements adsorption are given in Table 3.4. When the coefficients in chart are examined; interactions between sepiolite embedded composite cryogel and the elements all seem to be more appropriate for the pseudo second degree kinetic model. Adsorption capacity value achieved from pseudo-second order is compatible with experimental results. When the kinetic data were analyzed, it was obtained that the adsorption of sepiolite embedded composite cryogel elements was chemically controlled without any diffusion restriction.

Table 4.4. The pseudo 1st and 2nd order kinetic parameters calculated from kinetic analyses of the adsorption studies for 7 different elements.

	Experimental	**Pseudo-first order kinetic**			**Pseudo-second order kinetic**		
	Qe (µg/g)	**k_1 (1/min)**	**Qe (µg/g)**	**R^2**	**k_2 (mg/ml.min)**	**Qe (µg/g)**	**R^2**
Mn	0.5	0.018	2.29	0.5947	0.451	0.49	0.9978
Ni	0.55	0.015	2.16	0.7732	0.443	0.53	0.9987
As	0.35	0.012	2.17	0.7767	0.403	0.32	0.9985
Se	0.42	0.01	2.22	0.7978	0.602	0.37	0.9999
Cd	0.57	0.01	2.35	0.8568	0.818	0.52	0.9993
Sb	0.2	0.002	3.08	0.2804	9.960	0.14	0.9994
Co	0.54	0.013	2.09	0.6025	0.435	0.50	0.9984

4.7. Application to Certified Water

The certified multi-element standard solution contains 21 different elements (Table 4.5 and 4.6). Each element's initial concentrations in 1000 ppb solution are also shown in Table 4.5 and Table 4.6. Samples taken at the times specified earlier section of the heavy metal solution which interacted with the composite cryogel for 2 hours were detected by ICP-MS.

The concentration values and % adsorption values of the samples taken at each time were calculated according to Eq.1.

Table 4.5. Heavy metals in certified standard solution and their adsorption. % on composite cryogel (2 Hours, 1mL/min).

Heavy Metals	Initial Concentration (ppb)	Final Concentration (ppb)	Adsorption (%) of Sepiolite Embedded Cryogel
Cr	871.6	0	100
Mn	1025	134.8	86.84
Fe	401	0	100
Co	1015	89.36	91.19
Ni	1006	243.6	75.78
Cu	1020	211.9	79.22
Zn	1708	246.7	85.55
As	1149	283.9	75.29
Se	1271	606.2	52.30
Mo	1004	588.1	41.42
Cd	1095	69.23	93.67
Sb	1008	680	32.53

Table 4.6. Heavy metals in certified standard solution and their adsorption. % on composite cryogel (2 Hours, 1 mL/min).

Heavy Metals	Initial Concentration (ppb)	Final Concentration (ppb)	Adsorption (%) without Sepiolite Cryogel
Cr	861.5	658.5	23.56
Mn	947	657.5	30.57
Fe	588	454.75	22.66
Co	859.5	653	24.03
Ni	945	717.5	24.07
Cu	940	719.5	23.46
Zn	1285.5	1170	8.98
As	1052.5	807.5	23.28
Se	1298.5	1018.5	21.56
Mo	736	567.5	22.89
Cd	1058.5	827.5	21.82
Sb	972.5	773.5	20.46

Table 4.7. Comparison of adsorption in this thesis and other adsorption studies with cryogel.

LITERATURE COMPARISON								
Heavy Metals	**Removal Method**	**Heavy Metal Concentration**	**Adsorption Capacity**	**Research Groups**	**Ref.**	**Removal Method**	**Heavy Metal Concentration (ppb)**	**Adsorption on (%) of Sepiolite Embedded Cryogel**
Cd(II)	Cd(II) ion imprinted cryogels	100 ppm	13.91 mg/g	Jalilzadeh et al.	[110]	Sepiolite embedded nanocomposite cryogel	1095	93.67
Cu(II)	Cu(II) ion imprinted cryogels	100 ppm	11.20 mg/g	Jalilzadeh et al.	[110]	Sepiolite embedded nanocomposite cryogel	1020	79.22
As	Fe-Al cryogel	0.2 mg/L	24.6 mg/g	Önnby et al.	[111]	Sepiolite embedded nanocomposite cryogel	1149	75.29
Ni(II)	PHEMA-AC cryogel	20-300 mg/L	22 mg/g	Haktanır et al.	[112]	Sepiolite embedded nanocomposite cryogel	1006	75.78

Table 4.7. compares the removal methods of heavy metals with sepiolite embedded nanocomposite cryogels. According to Table 4.7, the heavy metals [Cd(II), Cu(II), As (III, V) and Ni(II)] adsorption capacities of sepiolite embedded nanocomposite cryogels were relatively high with regard to literature [110-112].

5. CONCLUSION

- Sepiolite tubular nanocrystals embedded composite cryogels were synthesized to efficiently remove heavy metals from the water solution.

- Composite cryogels offer significant potential for water treatment applications without clogging problems and medium flow resistance.

- In principle, the mutal effects between sepiolite nanocrystals and heavy metals have been considered in the process of complexation and polymerization. Therefore, composite cryogels exhibited high yield in the heavy metal removal.

- As stated in the results obtained, it would be very useful for multiple metal separation in aqueous medium.

- Synthesis of sepiolite embedded composite cryogel's advantages are capable to work with viscous and smooth liquids, such as wastewater, due their wide-pore structure.

- These liquids can flow through the sepiolite embedded cryogels. That properties simplified mass transfer, decreased the resistance of diffusion and their increased surface area provided us high binding efficiency.

- After the characterization studies of nanocomposite cryogels, their shapes have become spong-like elastic. Thus, even when pressure was applied such as hand compressing, they preserved their structure without disintegration.

- Composite cryogels was examined in the FTIR spectrum is between the values of 4000-600 cm^{-1}.

- The characteristic climax of sepiolite detected at 1436 cm^{-1}, which shows that the incorporation of the sepiolite into the S8 composite cryogel.

- According to SEM images, the interconnected pore structure of composite cryogels are between the values of 10-100 μM, layered structural image is formed after sepiolite enters the cryogel structure.

- Micro-computed tomography (μCT) analysis results showed that sepiolite embedded into the composite cryogels as impeccable.

- Cryogel's swelling degree balance was changed between 3.03-7.28 g H_2O/g cryogel by changing the crosslinker ratio.

- After tested with physical interventions it was seen that, cryogel containing sepiolite has a sponge-like elastic structure.

- After the adsorption experiments, the composite cryogel absorbed 97% of Cd and Co metals in water after 30 minutes. Maximum binding capacity were recorded at 30 min.

- The correlation coefficients of adsorption proces fit the Langmuir adsorption model for Mn, Ni, As, Se, Cd, Sb and Co. And also, Langmuir isotherm matches the experimental data.

- After the examined kinetic parameters, the adsorption of sepiolite embedded composite cryogel elements was chemically controlled without any diffusion restriction.

- Interactions between the heavy metals and composite cryogel are controlled chemically due to the interaction of heavy metal cations are through to the hydroxyl groups of sepiolites.

- The adsorption of heavy metal results showed us in this thesis study, heavy metal binding capacity of sepiolite embedded cryogels have amazing high efficiencies.

- >90% of Cr, Fe, Co, Zn and Cd metals were absorbed from water samples at 25°C in two hours by sepiolite embedded cryogels. But in the observed adsorption results showed us the sufficient time for maximum binding capacity is 30 minutes.

- Sepiolite embedded composite cryogels used as columns in this thesis study. Due to their flow resistance and durability, they can be used at high pressure flows and they can be produced almost in any shapes.

- Sepiolite embedded composite cryogels showed hihg efficiency for heavy metal removal, and materials, which are used in production and also production stages are low-cost.

- Considering the experiment studies and the results, sepiolite embedded composite cryogels have critical importance for heavy metalremoving from aqueous media.

REFERENCES

[1] P.B. Tchounwou, C.G. Yedjou, A.K. Patlolla, D.J. Sutton, Heavy Metals Toxicity and the Environment: EXS Journal, 133 (2012) 164.

[2] Z.L. He, X.E. Yang, P.J. Stoffella, Trace elements in agroecosystems and impacts on the environment: Journal of Trace Elements in Medicine and Biology, 125 (2005) 140.

[3] R.A. Goyer, Cassarett and Doull's Toxicology: The Basic Science of Poisons, C.D. Klaassen (Eds.), McGraw-Hill Publisher, New York, Chapter Toxic effects of metals, 811-867, 2001.

[4] M. Jaishankar, T. Tseten, N. Anbalagan, B. Mathew, K. Beeregowda, Toxicity, mechanism and health effects of some heavy metals: Interdiscip. Toxicol., 60 (2014) 72.

[5] E. Filiz, Doğal Kaynaklardan Elde Edilen Adsorbanlarla Sulardan Ağır Metal Giderimi, Yüksek Lisans Tezi, İstanbul Teknik Üniversitesi Fen Bilimleri Enstitüsü, İstanbul, 2007.

[6] B. Freedman, Environmental Ecology: The Ecological Effects of Pollution, Disturbance and Other Stresses, Academic Press, California, 1995.

[7] Ö. Kahvecioğlu, G. Kartal, A. Güven, S. Timur, Metallerin çevresel etkileri, Metalurji Dergisi, 47 (2009) 53.

[8] Ö. Ağcasulu, Sakarya Nehri Çeltikçe Çayı'nda Yaşayan Capoeta Tinca'nın Dokularında Ağır Metal Birikiminin İncelenmesi, Yüksek Lisans Tezi, Gazi Üniversitesi Fen Bilimleri Enstitüsü, Ankara, 2007.

[9] L. Jarup, Hazards of Heavy Metal Contamination, Br Med Bull, 167 (2003) 82.

[10] G.A. Engwa, P.U. Ferdinand, F.N. Nwalo, M.N. Unachukwu, Poisoning in the Modern World - New Tricks for an Old Dog?, Intechopen, Chapter:

Mechanism and Health Effects of Heavy Metal Toxicity in Humans, 1-2, 2019.

[11] C. Bakar, A. Baba, Metaller ve insan sağlığı: yirminci yüzyıldan bugüne ve geleceğe miras kalan çevre sağlığı sorunu, 1. Tıbbi Jeoloji Çalıştayı. 30 October- 1 November, Ürgüp, Nevşehir, 162-185, 2009.

[12] F. Fu, Q. Wang, Removal of heavy metal ions from wastewaters: A review: Journal of Environmental Management, 407 (2011) 418.

[13] Z.J. Rogers, S.A. Bencherif, Cryogelation and Cryogels: Gels, 1 (2019) 2.

[14] S. Muslumova, B. Yetişkin, O. Okay, Highly Stretchable and Rapid Self-Recoverable Cryogels Based on Butyl Rubber as Reusable Sorbent, Gels, Vol. 5, 1 (2019) 11.

[15] M. Bakhshpour, N. Idil, A. Denizli, Biomedical Applications of Polymeric Cryogels: Applied Sciences, 1 (2019) 17.

[16] K. Çetin, Moleküler Baskılanmış Kriyojel Disklerden Florourasil Salınımı, Yüksek Lisans Tezi, Hacettepe Üniversitesi Fen Bilimleri Enstitüsü, Ankara, 2013.

[17] K. Şarkaya, M. Bakhshpour, A. Denizli, Ag+ ions imprintedcryogels for selective removal of silver ions from aqueous solutions: Separation Science and Technology, 2993 (2018) 3004.

[18] B. Armagan, O. Ozdemir, M. Turhan, M.S. Celik, Clay Mineral Batch Process for Color Removal of Textile Wastewaters: Journal of Environmental Science and Health Part A, 2251 (2003) 2258.

[19] F. Wang, L. Feng, M. Tang, J. Li, Q. Tang, Advances in Water Treatment Application of Sepiolite Mineral Materials: Advanced Materials Research, 217 (2013) 220.

[20] A. Alvarez, Developments in Sedimentology, Palygorskite-Sepiolite. Occurrences, Genesis and Uses, A. Singer, E. Galán (Eds.), Vol. 37, Elsevier, Amsterdam, 266-283, 1984.

[21] H. İstanbulluoğlu, Piyasada satılan süt ve süt ürünlerinde ağır metal kirliliği, Uzmanlık tezi, Gülhane Askeri Tıp Akademisi, Ankara, 2011.

[22] L. Jarup, Hazards of heavy metal contamination: British Medical Bulletin, 167 (2003) 182.

[23] G. Özbolat, A. Tuli, Ağır Metal Toksisitesinin İnsan Sağlığına Etkileri, Arşiv Kaynak Tarama Dergisi, 502 (2016) 521.

[24] X.X. Long, X.E. Yang, W.Z. Ni, Current Status and Perspective on Phytoremediation of Heavy Metal Polluted Soils: Journal of Applied Ecology, 757 (2002) 762.

[25] ATSDR, Toxicological Profile for Copper, U.S. Department of Health and Humans Services, Public Health Service, Centers for Diseases Control, Atlanta, 2004.

[26] S.J. Banum, Introduction to Organic and Biological Chemistry, 3rd Edition, Macmillan Publishing Company, New York, 541, 1982.

[27] S. Morais, F.G. Costa, M.L. Pereira, Environmental Health - Emerging issues and practice, J. Oosthuizen (Eds.), IntechOpen, London, Chapter Heavy Metals and Human Health, 228, 2012.

[28] K . Thurmer, E. Williams, J. Reutt-Robey, Autocatalytic oxidation of lead crystallite surfaces: Science, 2033 (2002) 2035.

[29] M. Parmar, L.S. Thakur, Heavy Metal Cu, Ni and Zn: Toxicity, Health Hazards and Their Removal Techniques by Low Cost Adsorbents: A Short Overview: International Journal of Plant Sciences, 143 (2013) 157.

[30] Y.K. Chau, P.T.S. Wong, G.A. Bengert, Determination of tetraalkyl-lead compounds in water, sediments, and fish samples: Analytical Chemistry, 186 (1979) 188.

[31] ATSDR, Toxicological Profile for Lead, U.S. Department of Health and Humans Services, Public Health Service, Agency for Toxic Substances and Disease Registry, Atlanta, 2019.

[32] M.A. Oliver, Soil and Human Health: A review: European Journal of Soil Science, 573 (1977) 592.

[33] ATSDR, Toxicological Profile for Arsenic, U.S. Department of Health and Humans Services, Public Health Service, Agency for Toxic Substances and Disease Registry, Atlanta, 2019.

[34] K.S.M. Abdul, S.S. Jayasinghe, E.P.S. Chandana, C. Jayasumana, P.M.C.S. De Silva, Arsenic And Human Health Effects: A Review, 828 (2015) 846.

[35] N. Harrison, Inorganic Contaminants in Food, In: Food Chemical Safety Contaminants, D.H. Watson (Eds.), 1st Edition, Woodhead Publishing, Cambridge, 148-168, 2001.

[36] E. Figueroa, Are more restrictive food cadmium standards justifiable health safety measures or opportunistic barriers to trade? An answer from economics and public health: Science of the Total Environment 389, 1 (2008) 9.

[37] M. Unaegbu, G.A. Engwa, Q.D. Abaa, S.O. Aliozo, E.L. Ayuk, G.A. Osuji, Heavy metal, nutrient and antioxidant status of selected fruit samples sold in Enugu, Nigeria: International Journal of Food Contamination, 1 (2016) 8.

[38] A.G. Engwa, C.J. Ihekwoaba, U.S. Ilo, M. Unaegbu, L.E. Ayuk, A.G. Osuji, Determination of some soft drink constituents and contamination by some heavy metals in Nigeria, Toxicology Reports, Vol. 2, 384-390, 2015.

[39] M. Manohar, T. Shigaki, S. Shigaki, K. Hirschi, Past, Present and Future Approaches for Reducing Cadmium Content in Tobacco Leaves, 66th Tobacco Science Research Conference, At Concord, North Carolina, 2012, p. 9.

[40] ATSDR, Toxicological Profile for Cadmium, U.S. Department of Health and Humans Services, Public Health Service, Agency for Toxic Substances and Disease Registry, Atlanta, 2012.

[41] M.R. Rahimzadeh, M.R. Rahimzadeh, S. Kazemi, A. Moghadamnia, Cadmium toxicity and treatment: An update: Caspian Journal of Internal Medicine, 135 (2017) 145.

[42] M.I. Castro-González, M. Méndez-Armenta, Heavy metals: Implications associated to fish consumption: Environmental Toxicology & Pharmacology, 263 (2008) 271.

[43] J. Poulin, H. Gibb, Mercury: Assessing the Environmental Burden of Disease at National and Local Levels, A. Prüss-Üstün (Eds.), WHO, Geneva, 2008.

[44] ATSDR, Toxicological Profile for Mercury, U.S. Department of Health and Humans Services, Public Health Service, Agency for Toxic Substances and Disease Registry, Atlanta, 1999.

[45] A.E. Burakov, E.V. Galunin, I.V. Burakova, A.E. Kucherova, S. Agarwal, A.G. Tkachev, V.K. Gupta, Adsorption of heavy metals on conventional and nanostructured materials for wastewater treatment purposes: A review Ecotoxicology and Environmental Safety, 70.

[46] P. Ghosh, A.N. Samanta, S. Ray, Reduction of COD and removal of Zn2+ from rayon industry wastewater by combined electro-Fenton treatment and chemical precipitation: Desalination, 213 (2011) 217.

[47] Q.Y. Chen, Z. Luo, C. Hills, G. Xue, M. Tyrer, Precipitation of heavy metals from wastewater using simulated flue gas: sequent additions of fly ash, lime and carbon dioxide: Water Research, 2605 (2009) 2614.

[48] M.T. Alvarez, C. Crespo, B. Mattiasson,. Precipitation of Zn(II), Cu(II) and Pb(II) at bench-scale using biogenic hydrogen sulfide from the utilization of volatile fatty acids: Chemosphere 66, 1677 (2007) 1683.

[49] Z.R. Guo, G.M. Zhang, J.D. Fang, X.D. Dou, Enhanced chromium recovery from tanning wastewater: Journal of Cleaner Production, 75 (2006) 79.

[50] L.Y. Blue, M.A. Van Aelstyn, M. Matlock, D.A. Atwood, Low-level mercury removal from groundwater using a synthetic chelating ligand : Water Research, 2025 (2008) 2027.

[51] S.Y. Kang, J.U. Lee, S.H. Moon, K.W. Kim, Competitive adsorption characteristics of Co2+, Ni2+ and Cr3+ by IRN-77 cation exchange resin in synthesized wastewater: Chemosphere, 141 (2004) 147.

[52] K. Athanasiadis, B. Helmreich, Influence of chemical conditioning on the ion exchange capacity and on kinetic of zinc uptake by clinoptilolite: Water Research, 1527 (2005) 1532.

[53] M.E. Argun, Use of clinoptilolite for the removal of nickel ions from water: kinetics and thermodynamics: Journal of Hazardous Materials, 587 (2008) 595.

[54] V.J. Inglezakis, M.A. Stylianou, D. Gkantzou, M.D. Loizidou, Removal of Pb(II) from aqueous solutions by using clinoptilolite and bentonite as adsorbents: Desalination, 248 (2007) 256.

[55] M. Wołowiec, M.K. Kaufman, A. Pruss, G. Rzepa, T. Bajda, M. Wołowiec, M.K. Kaufman, A. Pruss, G. Rzepa, T. Bajda, Removal of Heavy Metals and Metalloids from Water Using Drinking Water Treatment Residuals as Adsorbents: A Review: Minerals, 1 (2019) 13.

[56] A.M. Shahalam, A. Al-Harthy, A. Al-Zawhry, Feed water pretreatment in RO systems in the Middle East: Desalination, 235 (2002) 245.

[57] B.K.C. Chan, A.W.L. Dudeney, Reverse osmosis removal of arsenic residues from bioleaching of refractory gold concentrates: Minerals Engineering, 272 (2008) 278.

[58] U.Ipek, Removal of Ni(II) and Zn(II) from an aqueous solution by reverse osmosis: Desalination, 161 (2005) 169.

[59] M. Mohsen-Nia, P. Montazeri, H. Modarress, Removal of Cu2+ and Ni2+ from wastewater with a chelating agent and reverse osmosis processes: Desalination, 276 (2007) 281.

[60] R. Molinari, T. Poerio, P. Argurio, Selective separation of copper(II) and nickel (II) from aqueous media using the complexationeultrafiltration process: Chemosphere, 341 (2008) 348.

[61] R. Camarilloa, J. Llanos, L.G. Fernández, Á. Pérez, P. Cañizares, Treatment of copper (II)-loaded aqueous nitrate solutions by polymer enhanced ultrafiltration and electrodeposition: Seperation and Purification Technology, 320 (2010) 328.

[62] U. Danisa, C. Aydiner, Investigation of process performance and fouling mechanisms in micellar-enhanced ultrafiltration of nickel-contaminated waters: Journal of Hazardous Materials, 577 (2009) 587.

[63] M.A. Barakat, E. Schmidt, Polymer-enhanced ultrafiltration process for heavy metals removal from industrial wastewater: Desalination, 90 (2010) 93.

[64] J.H. Huang, G.M. Zeng, C.F. Zhou, X. Li, L.J. Shi, S.B. He, Adsorption of surfactant micelles and Cd2+/Zn2+ in micellar-enhanced ultrafiltratio: Journal of Hazardous Materials, 287 (2010) 293.

[65] J.L. Aguirre, E. Pongrácz, P. Perämäk, R.L. Keiski, Micellarenhanced ultrafiltration for the removal of Cd and Zn: use of response surface methodology to improve understanding of process performance and optimisation: J. Hazard. Mater., 524 (2010) 534.

[66] F. Ferella, M. Prisciandaro, I.D. Michelis, F. Veglio, Removal of heavy metals by surfactant-enhanced ultrafiltration from wastewaters: Desalination, 125 (2007) 133.

[67] M. Sadrzadeha, T. Mohammadi, J. Ivakpour, N. Kasiri, Neural network modeling of Pb2+ removal from wastewater using electrodialysis: Chemical Engineering and Processing, 1371 (2009) 1381.

[68] S.K. Nataraj, K.M. Hosamani, T.M. Aminabhavi, Potential application of an electrodialysis pilot plant containing ion-exchange membranes in chromium removal: Desalination, 181 (2007) 190.

[69] S. Caprarescu, V. Purcar, A. Sârbu, A.L. Radu, M. Ghıurea, I. Maıor, The Use of Electrodıalysıs for Cu2+ Removal from Wastewater: Academıa Română, 639 (2014) 644.

[70] P. Mikulasek, J. Cuhorka, Removal of heavy metals ions from aqueous solutions by nanofiltration, Chemical Engineering Transactions, 379 (2016) 384.

[71] J.Tanninen, M. Mänttäri, M. Nyström,. Nanofiltration of concentrated acidic copper sulphate solutions: Desalination, 92 (2006) 96.

[72] T. Chaabane, S. Taha, M. Taleb Ahmed, R. Maachi, G. Dorange, Removal of copper from industrial effluent using a spiral wound module d film theory and hydrodynamic approach: Desalination, 403 (2006) 405.

[73] A. Figoli, A. Cassano, A. Criscuoli, M.S.I. Mozumder, M.T.Uddin, M.A. Islam, E. Drioli, Influence of operating parameters on the arsenic removal by nanofiltration: Water Research, 97 (2010) 104.

[74] Z.V.P. Murthy, L.B. Chaudhari, Application of nanofiltration for the rejection of nickel ions from aqueous solutions and estimation of membrane transport parameters: Journal of Hazardous Materials, 70 (2008) 77.

[75] Anonim, Electrodeposition, https://wwwfr.uni.lu/recherche/fstm/dphyms/research_areas/photovoltaics/research/electrodeposition (Erişim tarihi: 9 Şubat 2020).

[76] A. Khelifa, S. Moulay, A.W. Naceur, Treatment of metal finishing effluents by the electroflotation technique: Desalination, 27(2005) 33.

[77] R.G. Casqueira, M.L. Torem, H.M. Kohler, The removal of zinc from liquid streams by electroflotation: Minerals Engineering, 1388 (2006) 1392.

[78] T. Ölmez, The optimization of Cr(VI) reduction and removal by electrocoagulation using response surfacemethodology: Journal of Hazardous Materials,1371 (2009) 1378.

[79] J.R. Parga, D.L. Cocke, J.L. Valenzuela, J.A. Gomes, M. Kesmez, G. Irwin, H. Moreno, M. Weir, Arsenic removal via electrocoagulation from heavy metal contaminated groundwater in La Comarca Lagunera México: Journal of Hazardous Materials, 247 (2005) 254.

[80] A. Shafaei, M. Rezayee, M. Arami, M. Nikazar, Removal of Mn2+ ions from synthetic wastewater by electrocoagulation process: Desalination, 23 (2010) 28.

[81] J.H. Chang, A.V. Ellis, C.T. Yan, C.H. Tung, The electrochemical phenomena and kinetics of EDTA-copper wastewater reclamation by electrodeposition and ultrasound: Seperation and Purification Technology, 216 (2009) 221.

[82] J. Saleem, U.B. Shahid, M. Hijab, H. Mackey, G. McKay, Production and applications of activated carbons as adsorbents from olive stones: Biomass Conversion and Biorefinery, 775 (2019) 802.

[83] D. Obregón-Valencia , R.M. del Sun-Kou, Comparative cadmium adsorption study on activated carbon prepared from aguaje (Mauritia flexuosa) and olive fruit stones (Olea europaea L.): Journal of Environmental Chemical Engineering, 2280 (2014) 2288.

[84] P. Galiatsatou, M. Metaxas, V. Kasselouri-Rigopoulou, Adsorption of zinc by activated carbons prepared from solvent extracted olive pulp: Journal of Hazardous Materials, 187 (2002) 203.

[85] T. Bohli, A. Ouederni, N. Fiol, I. Villaescusa, Single and binary adsorption of some heavy metal ions from aqueous solutions by activated carbon derived from olive stones: Desalination and Water Treatment, 1 (2013) 7.

[86] Y.H. Li, Y.M. Zhao, W.B. Hu, I. Ahmad, Y.Q. Zhu, X.J. Peng, Z.K. Luan, Carbon nanotubes – the promising adsorbent in wastewater treatment: Journal of Physics Conference Series, 698 (2007) 702.

[87] A. Sadeghinya, B. Bina, A.H. Mahvi, A. Esrafili, E. Dehghanifard, L.K. Takanlu, Efficiency determination of single-walled carbon nanotubes on adsorption of copper ions from synthetic wastewater: Int. J. Env. Health Eng., 1 (2015) 6.

[88] F. Golbabaei, A. Ebrahimi, H. Shirkhanloo, A. Koohpaei, A. Faghihi-Zarandi, Single-Walled Carbon Nanotubes (SWCNTs) as a Novel Sorbent for Determination of Mercury in Air: Global Journal of Health Science, 273 (2016) 280.

[89] Ana Rita Lino Oliveira,Heavy metal ions removal from aqueous solutions byMultiwalled Carbon Nanotubes, Master's Thesis, University of Coimbra Faculty of Science and Technology, Coimbra, 2016.

[90] T.A. Davis, B. Volesky, A. Mucci, A review of the biochemistry of heavy metal biosorption by brown algae: Water Research, 4311 (2003) 4330.

[91] A. Rathinam, B. Maharshi, S.K. Janardhanan, R.R. Jonnalagadda, B.U. Nai, Biosorption of cadmium metal ion from simulated wastewaters using Hypnea valentiae biomass: A kinetic and thermodynamic study: Bioresource Technology, 1466 (2010) 1470.

[92] P. SenthilKumar, S. Ramalingam, V. Sathyaselvabala, S.D. Kirupha, S. Sivanesan, Removal of copper (II) ions from aqueous solution by adsorption using cashew nut shell: Desalination, 63 (2011) 71.

[93] A.G. El Samrani, B.S. Lartiges, F. Villiéras, Chemical coagulation of combined sewer overflow: heavy metal removal and treatment optimization: Water Research, 951 (2008) 960.

[94] Q. Chang, M. Zhang, J.X. Wang, Removal of Cu2+ and turbidity from wastewater by mercaptoacetyl chitosan: Journal of Hazardous Materials, 621 (2009) 625.

[95] F.M. Pang, P. Kumar, T.T. Teng, A.K.M. Omar, K.L. Wasewar, Removal of lead, zinc and iron by coagulation–flocculation: Journal of the Taiwan Institute of Chemical Engineers, 809 (2011) 815.

[96] A. Cronstedt, Versuch Einer Neuen Mineralogie, Stockholm, Sect.84, 89-90, 1760.

[97] A. Cronstedt, An Essay Towards A System Of Mineralogy, (çev: J.H. De Magellan), London, Sect.133, 235-237, 1788.

[98] A.G. Werner, Letztes Mineral-System, Graz und Gerlach, 82, 1809.

[99] J.D. Dana, A System Of Mineralogy, 2nd Edition, Wiley and Putnam, 308, 1844.

[100] E.F. Glocker, Generum et Specierum Mineralium Secundum Ordines Naturales Digestorium Synopsis, E. Anton, 190, 1847.

[101] F. Bergaya, K. Beneke, G. Lagaly, History and Perspectives of Clay Science, vol. 4, ECGA News-Letter, Nehmten, Germany, 16, 2001.

[102] E. Sabah, O. Özdemir, B. Armağan, M.S. Çelik, Elımınatıon Of Pollutants In Wastewater By Sepıolıte, EPMR-2002 International Conference, April, North Cyprus, Turkey, 1-9, 2002.

[103] M. Doğan, Y. Turhan, M. Alkan, H. Namli, P. Turan, Ö. Demirbaş Functionalized sepiolite for heavy metal ions adsorption: Desalination, 248 (2008) 268.

[104] Z. Wang, L. Liao, A. Hursthouse, N. Song, B. Ren, Sepiolite-Based Adsorbents for the Removal of Potentially Toxic Elements from Water: Int. J. Env. Res. Pub. Health, 1 (2018) 15.

[105] F.A.C. Smirnov, O. Piétrement, P. Aranda, J.R. Bertrand, J. Ayache, E.L. Cam, E.R. Hitzky, B.S. Lopez, Physical interactions between DNA and sepiolite nanofibers, and potential application for DNA transfer into mammalian cells: Sci. Rep., 1 (2016) 14.

[106] R. Celis, M.C. Hermosín, J. Cornejo, Heavy Metal Adsorption by Functionalized Clays: Environmental Science Technology, 4593 (2000) 4599.

[107] M. Darder, M.L. Blanco, P. Aranda, A.J. Aznar, J. Bravo, E.R. Hitzky, Microfibrous Chitosan-Sepiolite Nanocomposites: Chem. Mater., 1602 (2006) 1610.

[108] K. Fukushima, D. Tabuani, G. Camino, Nanocomposites of PLA and PCL based on montmorillonite and sepiolite: Materials Science and Engineering C, 1433 (2009) 1441.

[109] A.K. Nayak, B. Das, Introduction to polymeric gels, in Polymeric gels characterization, properties and biomedical applications, K. Pal, I. Bannerjee (Eds.),A volume in Woodhead Publishing Series in Biomaterials, Elsevier Ltd., 22, 2018.

[110] F.M. Plieva, I.N. Savina, S. Deraz, J. Andersson, I.G. Galaev, B. Mattiasson, Characterization of supermacroporous monolithic polyacrylamide based matrices designed for chromatography of bioparticles: J. Chromatogr. B, 129 (2004) 137.

[111] M. Andac¸ I.Y. Galaev, A. Denizli, Affinity based and molecularly imprinted cryogels: Applications inbiomacromolecule purification: Journal of Chromatography B, 69 (2016) 80.

[112] S. Asliyuce, L. Uzun, A.Y. Rad, S. Unal, R. Say, R. Denizli, Molecular imprinting based composite cryogel membranes for purification of anti-hepatitis B surface antibody by fast protein liquid chromatography: J. Chromatogr. B, 95 (2012) 102.

[113] F.M. Plieva, M. Karlsson, M.R. Aguilar, D. Gomez, S. Mikhalovsky, I.Y. Galaev, Pore structure in supermacroporous polyacrylamide based cryogels, Soft Matter, Vol. 1, 303 (2005) 309.

[114] V. Lozinsky, F. Plieva, I. Galaev and B. Mattiasson, The potential of polymeric cryogels in bioseparation, Bioseparation, Vol. 10, 163 (2001) 188.

[115] A. Al-Abboodi, J. Fu, P.M. Doran, P.P.Y. Chan, Three-dimensional nanocharacterization of porous hydrogel with ion and electron beams:Biotechnol. Bioeng., 318 (2013) 326.

[116] V.I. Lozinsky, E.S. Vainerman, S.A. Ivanova, E.F. Titova, M.I. Shtil'man, E.M. Belavtseva, S.V. Rogozhin, Study of cryostructurization of polymer systems, Acta Polymerica, Vol. 37, 142 (1986) 146.

[117] A. Fatoni, A. Numnuam, P. Kanatharana, W. Limbut, P. Thavarungkul, A novel molecularly imprinted chitosan–acrylamide, graphene, ferrocene composite cryogel biosensor used to detect microalbumin: Analyst, 6160 (2014) 6167.

[118] M. Uygun, A.A. Karagözler, A. Denizli, Molecularly imprinted cryogels forcarbonic anhydrase purification from bovine erythrocyte: Artif. CellsNanomed. Biotechnol., 128 (2014) 137.

[119] I. Inci, H. Kirsebom, I.Y. Galaev, B. Mattiasson, E. Piskin, Gelatin cryogels crosslinked with oxidized dextran and containing freshly formed hydroxyapatite as potential bone tissue-engineering scaffolds: J. Tissue Eng. Regener. Med., 548 (2012) 588.

[120] S. Nilsang, V. Nehru, F.M. Plieva, K.S. Nandakumar, S.K. Rakshit, R. Holmdahl, B. Mattiasson, A. Kumar, 3-D culture for monoclonal antibodyproduction by hybridoma cells Immobilized in macroporous gelparticles: Biotechnol. Prog., 1122 (2008) 1131.

[121] A. Derazshamshir, G. Baydemir, M. Andac, R. Say, I.Y. Galaev, A. Denizli, Molecularly imprinted phema-based cryogel for depletion of hemoglobin from human blood: Macromol. Chem. Phys., 657 (2010) 668.

[122] M. Jalilzadeh, Desıgnıng Of Ion-Imprınted Cryogels And Theır Use For Heavy Metal Removal, Partial Fulfillment to the Requirements for the

Award of the Degree of Doctor of Philosophy in Chemistry, Institute of Science of Hacettepe University, Ankara, 2014.

[123] L. Önnby, Water treatment using cryogel-based adsorbents - Targeting environmental pollutants at low concentrations, Doctoral Dissertation, Department of Biotechnology in Lund University, Sweden, 2013.

[124] C. Haktanır, Removal of Heavy Metals From Aqueus Solution Using Activated Carbon Embedded Cryogels: Hacettepe J. Biol. & Chem., 135 (2017) 142.

[125] K.Y. Foo, B.H. Hameed, Insights into the Modeling of Adsorption Isotherm Systems, Chemical Engineering Journal, 2 (2010) 10.

[126] A.C. Parmeggiani, J.C. Masini, Evaluating Scatchard and Differential Equilibrium Functions to Study The Binding Properties of Cu(II) to The Surface of Mixed Species of lyophilized Spirulina (Cyanobacteria), J. Braz. Chem. Soc., 416 (2003) 424.

[127] D. Robati, Pseudo-Second-Order Kinetic Equations for Modeling Adsorption Systems for Removal of Lead Ions Using Multi-Walled Carbon Nanotube, J. Nanostruct. Chem., 1 (2013) 6.

[128] L. Largitte, R. Pasquier, A Review of The Kinetics Adsorption Models and Their Application to The Adsorption of Lead by An Activated Carbon, Chem. Eng. Research and Design, 495 (2016) 504.

[129] F.M. Plieva, K.A. Kochetkov, I. Singh, V.S. Parmar, Y.N. Belokon, V.I. Lozinsky, Immobilization of hog pancreas lipase in macroporous poly(vinylalcohol)-cryogel carrier for the biocatalysis in water-poor media: Biotechnology Letters, 551 (2000) 554.

[130] M. Andac, I.Y. Galaev, A. Denizli, Molecularlyimprintedpoly(hydroxyethylmethacrylate)basedcryogelforalbumindepletionfromhumanserum: Colloids and Surfaces B: Biointerfaces, 259 (2013) 265.

HACETTEPE UNIVERSITY
GRADUATE SCHOOL OF SCIENCE AND ENGINEERING
THESIS/DISSERTATION ORIGINALITY REPORT

HACETTEPE UNIVERSITY
GRADUATE SCHOOL OF SCIENCE AND ENGINEERING
TO THE DEPARTMENT OF ENVIRONMENTAL ENGINEERING

Date: 13/07/2020

Thesis Title / Topic: Sepiolite Embedded Nanocomposite Cartridges for Heavy Metal Removal from Water

According to the originality report obtained by myself/my thesis advisor by using the *Turnitin* plagiarism detection software and by applying the filtering options stated below on 13/07/2020 for the total of 96 pages including the a) Title Page, b) Introduction, c) Main Chapters, d) Conclusion sections of my thesis entitled as above, the similarity index of my thesis is 10 %.

Filtering options applied:

1. Bibliography/Works Cited excluded
2. Quotes excluded
3. Match size up to 5 words excluded

I declare that I have carefully read Hacettepe University Graduate School of Sciene and Engineering Guidelines for Obtaining and Using Thesis Originality Reports; that according to the maximum similarity index values specified in the Guidelines, my thesis does not include any form of plagiarism; that in any future detection of possible infringement of the regulations I accept all legal responsibility; and that all the information I have provided is correct to the best of my knowledge.

I respectfully submit this for approval.

Date and Signature
13/07/2020

Name Surname: Çağtay ÇİÇEK
Student No: N17127689
Department: Environmental Engineering
Program:
Status: ☒ Masters ☐ Ph.D. ☐ Integrated Ph.D.

ADVISOR APPROVAL

APPROVED.

Assoc. Prof. A. Müge ANDAÇ ÖZDİL

(Title, Name Surname, Signature)

RESUME

Name and Surname : ÇAĞTAY ÇİÇEK
Place of birth : KIRIKKALE
Date of birth : 02/12/1990
Adress : Kaletepe Mah. Genç Osman Cad. Yaren Apt. No: 15D:10 Kırıkkale
Phone number : +90 (553) 583 60 71
E-mail address : cagtay_cicek@outlook.com
Foreign language : English

EDUCATION STATUS:

Bachelor : Environmental Science, Akdeniz University
Master : Environmental Science, Hacettepe University

WORK EXPERIENCE

2010 Internship	TPA Company / İzmir 90 Days of Work
2011 Internship	MKE / Kırıkkale 30 Days of Work
2012 Internship	ASAT Lara / Antalya 30 Days of Work
2013 Internship	ILBANK / Antalya 30 Days of Work
2016 Work	Alsancak Group Security & Consultancy Co. Ltd. Administrative Asistant(Correspondence and Preparation of Business Documents in English) 60 Days of Work

2017 Internship	Hacettepe University Biochemistry Laboratory Experimental Field
2018 Work	Botek Ar-Ge Kimya A.Ş. Environmental Eng. (Project Developer for heavy metal removal from aqueous) (7 Months, Ended in May)

CERTIFICATES

- TC Environmental and Urban Ministry - Çevre Görevlisi Belgesi
- English Language Certificate / American Culture
- Selçuk University Organization and Meeting Community Career of Consciousness Certificate
- GIWEH – Global Institute for Water, Environment and Health Certificate
- Hacettepe University - Certificate of Affinity Bases on Sensors